

AD-A103 928

ILLINOIS UNIV AT URBANA COORDINATED SCIENCE LAB
RESEARCH TO PROVIDE A THEORETICAL DETERMINATION OF SURFACE ACOU--ETC(U)
JUL 81 B J HUNSINGER

F/G 9/3

F19628-78-C-0040

NL

UNCLASSIFIED

RADC-FR-81-175

1 OF 1
ADA-A
019628

END
DATA FILMED
1-B-01
DTIC

ADA103928

(18) RADC TR-81-173

Final Technical Report

(19) July 1981

(11)

LEVEL

(12) A097337

(13) 11

(14) Final rept.

(15) 6

(16) 1

(17) 3

(18) 4

(19) 5

(20) 6

(21) 7

(22) 8

(23) 9

(24) 10

(25) 11

(26) 12

(27) 13

(28) 14

(29) 15

(30) 16

(31) 17

(32) 18

(33) 19

(34) 20

(35) 21

(36) 22

(37) 23

(38) 24

(39) 25

(40) 26

(41) 27

(42) 28

(43) 29

(44) 30

(45) 31

(46) 32

(47) 33

(48) 34

(49) 35

(50) 36

(51) 37

(52) 38

(53) 39

(54) 40

(55) 41

(56) 42

(57) 43

(58) 44

(59) 45

(60) 46

(61) 47

(62) 48

(63) 49

(64) 50

(65) 51

(66) 52

(67) 53

(68) 54

(69) 55

(70) 56

(71) 57

(72) 58

(73) 59

(74) 60

(75) 61

(76) 62

(77) 63

(78) 64

(79) 65

(80) 66

(81) 67

(82) 68

(83) 69

(84) 70

(85) 71

(86) 72

(87) 73

(88) 74

(89) 75

(90) 76

(91) 77

(92) 78

(93) 79

(94) 80

(95) 81

(96) 82

(97) 83

(98) 84

(99) 85

(100) 86

(101) 87

(102) 88

(103) 89

(104) 90

(105) 91

(106) 92

(107) 93

(108) 94

(109) 95

(110) 96

(111) 97

(112) 98

(113) 99

(114) 100

(115) 101

(116) 102

(117) 103

(118) 104

(119) 105

(120) 106

(121) 107

(122) 108

(123) 109

(124) 110

(125) 111

(126) 112

(127) 113

(128) 114

(129) 115

(130) 116

(131) 117

(132) 118

(133) 119

(134) 120

(135) 121

(136) 122

(137) 123

(138) 124

(139) 125

(140) 126

(141) 127

(142) 128

(143) 129

(144) 130

(145) 131

(146) 132

(147) 133

(148) 134

(149) 135

(150) 136

(151) 137

(152) 138

(153) 139

(154) 140

(155) 141

(156) 142

(157) 143

(158) 144

(159) 145

(160) 146

(161) 147

(162) 148

(163) 149

(164) 150

(165) 151

(166) 152

(167) 153

(168) 154

(169) 155

(170) 156

(171) 157

(172) 158

(173) 159

(174) 160

(175) 161

(176) 162

(177) 163

(178) 164

(179) 165

(180) 166

(181) 167

(182) 168

(183) 169

(184) 170

(185) 171

(186) 172

(187) 173

(188) 174

(189) 175

(190) 176

(191) 177

(192) 178

(193) 179

(194) 180

(195) 181

(196) 182

(197) 183

(198) 184

(199) 185

(200) 186

(201) 187

(202) 188

(203) 189

(204) 190

(205) 191

(206) 192

(207) 193

(208) 194

(209) 195

(210) 196

(211) 197

(212) 198

(213) 199

(214) 200

(215) 201

(216) 202

(217) 203

(218) 204

(219) 205

(220) 206

(221) 207

(222) 208

(223) 209

(224) 210

(225) 211

(226) 212

(227) 213

(228) 214

(229) 215

(230) 216

(231) 217

(232) 218

(233) 219

(234) 220

(235) 221

(236) 222

(237) 223

(238) 224

(239) 225

(240) 226

(241) 227

(242) 228

(243) 229

(244) 230

(245) 231

(246) 232

(247) 233

(248) 234

(249) 235

(250) 236

(251) 237

(252) 238

(253) 239

(254) 240

(255) 241

(256) 242

(257) 243

(258) 244

(259) 245

(260) 246

(261) 247

(262) 248

(263) 249

(264) 250

(265) 251

(266) 252

(267) 253

(268) 254

(269) 255

(270) 256

(271) 257

(272) 258

(273) 259

(274) 260

(275) 261

(276) 262

(277) 263

(278) 264

(279) 265

(280) 266

(281) 267

(282) 268

(283) 269

(284) 270

(285) 271

(286) 272

This report has been reviewed by the RADC Public Affairs Office (PA) and is releasable to the National Technical Information Service (NTIS). At NTIS it will be releasable to the general public, including foreign nations.

RADC-TR-81-173 has been reviewed and is approved for publication.

APPROVED:



ANDREW J. SLOBODNIK, Jr.
Project Engineer

APPROVED:



ALLAN C. SCHELL
Chief, Electromagnetic Sciences Division

FOR THE COMMANDER:



JOHN P. HUSS
Acting Chief, Plans Office

If your address has changed or if you wish to be removed from the RADC mailing list, or if the addressee is no longer employed by your organization, please notify RADC (EEA) Hanscom AFB MA 01731. This will assist us in maintaining a current mailing list.

Do not return this copy. Retain or destroy.

UNCLASSIFIED

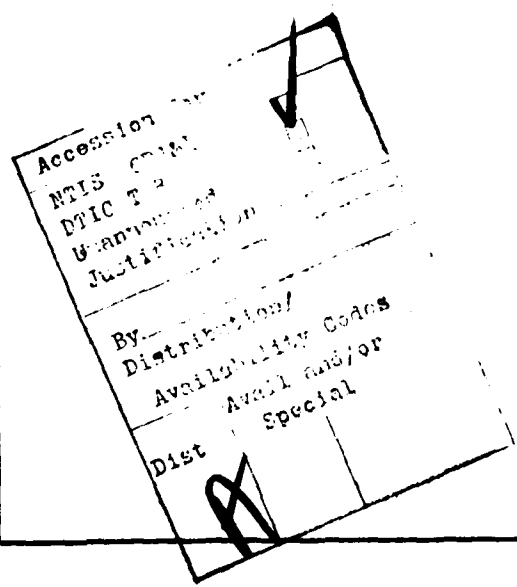
SECURITY CLASSIFICATION OF THIS PAGE (When Data Entered)

REPORT DOCUMENTATION PAGE		READ INSTRUCTIONS BEFORE COMPLETING FORM
1. REPORT NUMBER RADC-TR-81-173 ✓	2. GOVT ACCESSION NO. <i>AD-R103 928</i>	3. RECIPIENT'S CATALOG NUMBER
4. TITLE (and Subtitle) RESEARCH TO PROVIDE A THEORETICAL DETERMINATION OF SURFACE ACOUSTIC WAVE VELOCITY AND IMPEDANCE DIFFERENCES BETWEEN METAL STRIPS AND FREE SURFACE REGIONS OF METALLIC GRATINGS		5. TYPE OF REPORT & PERIOD COVERED Final Technical Report
7. AUTHOR(s) B. J. Hunsinger	6. PERFORMING ORG. REPORT NUMBER N/A	
		8. CONTRACT OR GRANT NUMBER(s) F19628-78-C-0040 ✓
9. PERFORMING ORGANIZATION NAME AND ADDRESS Coordinated Science Laboratory University of Illinois at Urbana-Champaign 1101 W. Springfield Ave, Urbana IL 61801		10. PROGRAM ELEMENT, PROJECT, TASK AREA & WORK UNIT NUMBERS 61102F 2305J524
11. CONTROLLING OFFICE NAME AND ADDRESS Deputy for Electronic Technology (RADC/EEA) Hanscom AFB MA 01731		12. REPORT DATE July 1981
		13. NUMBER OF PAGES 50
14. MONITORING AGENCY NAME & ADDRESS (if different from Controlling Office) Same		15. SECURITY CLASS. (of this report) UNCLASSIFIED
		15a. DECLASSIFICATION/DOWNGRADING SCHEDULE N/A
16. DISTRIBUTION STATEMENT (of this Report) Approved for public release; distribution unlimited.		
17. DISTRIBUTION STATEMENT (of the abstract entered in Block 20, if different from Report) Same		
18. SUPPLEMENTARY NOTES RADC Project Engineer: Andrew J. Slobodnik, Jr. (EEA)		
19. KEY WORDS (Continue on reverse side if necessary and identify by block number) Surface Acoustic Waves (SAW) SAW Gratings SAW Velocity Differences SAW Transducer Analysis SAW Impedance Differences Low Reflection SAW Transducers		
20. ABSTRACT (Continue on reverse side if necessary and identify by block number) With the advent of surface acoustic wave resonators and withdrawal weighted filters, quantitative knowledge of the velocity and acoustic impedance differences between metal strips and free surface regions in metallic gratings used for these structures has become necessary. During the course of this program mass loading, topographical effects, electrical loading, and energy storage have been considered and the surface acoustic wave velocity and impedance differences (DETERV and DELTERZ) have been		

UNCLASSIFIED

SECURITY CLASSIFICATION OF THIS PAGE(When Data Entered)

theoretically determined for shorted arrays, single electrode transducers and double electrode transducers at center frequency. Buried electrodes are also considered. It was an objective to find the electrode structure that produced the minimum impedance and velocity perturbation. It has been found that acoustic impedance mismatch and velocity shift, unlike in a transmission line, are not minimized simultaneously. Combinations of electrode metals are suggested for minimizing each of the perturbations. The results are presented in a form that is useful in the transmission line model analysis of SAW devices.



UNCLASSIFIED

SECURITY CLASSIFICATION OF THIS PAGE(When Data Entered)

TABLE OF CONTENTS

I.	Overview	1
A.	Objective	
B.	Approach	
II.	One electrode in an infinite array	5
A.	Equivalent transmission line parameters and general introduction	
B.	Piezoelectric scattering	
C.	First order mechanical scattering	
D.	Second order mechanical scattering	
E.	Additional dicussion on bimetal electrodes	
F.	Buried electrodes	
III.	Finite array analysis	33
A.	Physical interpretation of neighboring electrode effects	
1.	Piezoelectric scattering	
2.	First order mechanical scattering	
3.	Second order mechanical scattering	
B.	Finite array parameters defined in terms of infinite array parameters	
IV.	Low perturbation bimetal electrodes	39
A.	Cancellation of piezoelectric scattering by mechanical scattering	
B.	Low impedance mismatch for single electrode transducers	
C.	Low velocity shift in double electrode transducers	
V.	Summary and Conclusions	45
Appendix: Finite array effects on second order mechanical scattering . . .		49

Section I: Overview

A. Objective

Surface acoustic wave transducers and reflectors are frequently modelled using a transmission line equivalent circuit. Thin electrodes and shallow grooves located in the surface acoustic wave propagation path produce reflections and shift the propagation velocity of the wave. The effect of the electrodes and grooves are modelled as an offset in characteristic impedance (DELTERZ) and a shift in the propagation velocity (DELTERV) [1]. In this program a theoretical analysis was developed to calculate this impedance offset and velocity shift from the material constants and the geometrical dimensions considering both the mechanical and the electrical loading of the surface. The detailed theory has been published in a series of papers during the course of the development [2-9]. This report is written to tie these studies together and to provide a compact summary of the results that will be useful to the device designer. The detailed derivations are contained in the references and are left out of this report in order to make it a better design tool.

B. Approach

The total charge induced by an acoustic wave in an electrode loaded with a finite impedance can be broken into two parts. An incident SAW induces a voltage across the electrodes if they are connected through a finite impedance. The charge resulting from this voltage is calculated using transducer theory [10]. However, a shorted electrode excited by an acoustic wave also has charge induced upon it though there is no voltage. Transducer theory does not account for this component of the charge. In addition, the

mass and elasticity of the electrode structures react against the displacement of the wave and produce a set of stresses near the surface. These charges and stresses work together as an effective surface wave generating transducer which produces both forward and reverse traveling waves. The forward traveling waves add vectorially with the incident wave to change its phase; this is interpreted as an effective velocity shift. The reverse wave appears as a reflection and is therefore modelled by the transmission line equivalent circuit as an impedance mismatch element. In this paper we provide these parameters for a SAW propagating under a series of shorted electrodes. The additional charge due to a finite impedance load is already accounted for by transducer theory.

The forward and reverse waves generated by the stress patterns of the mechanical loading and the charge distributions of the electrical loading are calculated separately and added to provide the overall effect. The fact that the elastic and electrical scattering may be calculated separately should not be surprising when one remembers that both effects are small. A numerical analysis which considered all effects simultaneously was generated during the first year of the this program. This analysis verified that one gets the same results if the elastic and electrical locations are considered separately as long as the perturbations are less than a few percent per wave length. This is an important realization because considering these effects separately simplifies the analysis and makes results more useful to the device designer.

Both the elastic and the piezoelectric loading are made up of two components, each of which can be calculated separately.

- (1) The first order mechanical scattering (FOMS) is the result of the electrode mass and elasticity working against a rigid substrate.

- (2) The second order mechanical scattering (SOMS) is a result of substrate distortion produced by the electrode. This scattering is commonly called the "stored energy effect" in the literature.
- (3) The shorted array piezoelectric scattering (PS) is the result of charge being induced on a series of grounded electrodes when an incident SAW is present.
- (4) The regenerated wave piezoelectric scattering (RWS) is the result of voltages being induced on an IDT connected to a finite electric load.

Each of these scattering mechanisms give rise to reflections and velocity shifts. This report provides a DELTERZ to account for reflections and a DELTERV to account for velocity shift. A DELTERZ and a DELTERV are provided for FOMS, SOMS, and PS. The transmission line model accounts for the RWS and no DELTERZ and DELTERV are required for that type of scattering.

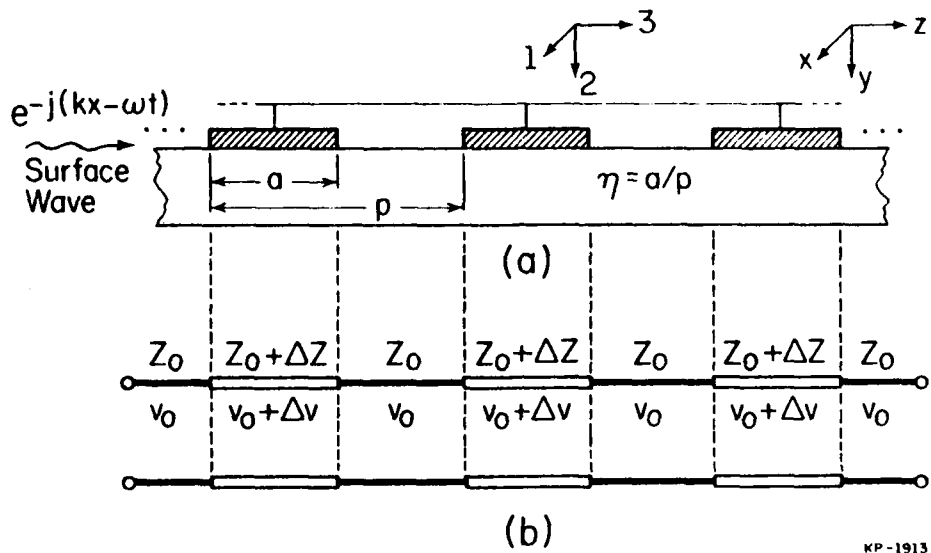
If a typical electrode thickness of about $.01 \lambda$ is used, the PS is the dominant effect for the strong coupling coefficient materials such as YZ lithium niobate. With split finger aluminum electrodes on ST Quartz, the PS and FOMS are small when compared to the SOMS.

This analysis is also good for grooves and buried electrodes. Grooves are analyzed as a substrate loaded with dielectric electrodes (only FOMS and SOMS are considered) sized and located to produce the topography of the surface. Buried electrode transducers are analyzed as the metal electrodes interleaved with dielectric electrodes. When the DELTERZ and DELTERV for each type of scattering and electrode are placed appropriately into the transmission line model, the result is a composite model that gives accurate results as long as each of the perturbations is small.

The velocity shift and impedance mismatch arising from ROMS have been derived in Reference 3 and the results are also written out in terms of analytical expressions that give DELTERV and DELTERZ in terms of material constants and geometrical dimensions. The SOMS is a more complicated analysis described in References 4 and 5. The results are in the form of a matrix equation involving the material parameters and the geometrical dimensions. However, the matrix equation must be solved numerically and simple analytical expressions are not practical. The PS has been described as closed form analytical expressions which are published in Reference 2.

Section II: One electrode in an infinite array

A. Equivalent transmission line parameters and general introduction



KP-1913

Figure 1: Surface Wave Propagation in a Periodic Array

(a) Actual Configuration

(b) Equivalent Transmission Line

The objective of this section is to determine the equivalent transmission line parameters required to model the propagation of Surface Acoustic Waves (SAW) in an infinite periodic array of shorted metallic electrodes. In this model, the wave velocity, v_0 , in the gaps is equal to the surface wave velocity along a free surface, while under the electrodes it has a different

value, $v_0 + \Delta v$ (Fig. 1). The characteristic impedance, too, is different in the gaps (Z_0) and under the electrodes ($Z_0 + \Delta Z$). The purpose of this program is to determine the fractional velocity shift $\Delta v/v_0$ and the impedance mismatch $\Delta Z/Z_0$ starting from the material parameters (stiffness, piezoelectric constant and permittivity) of the substrate and the electrodes. These values ($\Delta v/v_0$ and $\Delta Z/Z_0$) can then be used in a transmission line model for the analysis and design of SAW transducers.

The effective coupling constant K^2 for surface waves is defined as twice the fractional velocity shift due to an infinitely long conductive layer (with negligible thickness and negligible mass) at the surface. In this idealized situation and if the surface wave were a usual one-dimensional plane wave in a transmission line, we would expect:

$$\frac{\Delta v}{v_0} = -\frac{K^2}{2} \quad (1a)$$

$$\frac{\Delta Z}{Z_0} = -\frac{K^2}{2} \quad (1b)$$

However, the surface wave is not a plane wave; it is far more complicated with acoustic (shear and compressional) fields coupled together. In addition, physical electrodes have both thickness and mass. As a result, the actual $\Delta v/v_0$ and $\Delta Z/Z_0$ are different from the simple results in Equations (1). These differences or "correction terms" are defined as DELTERV and DELTERZ:

$$\frac{\Delta v}{v_0} = -\frac{k^2}{2} - \text{DETERV} \quad (2a)$$

$$\frac{\Delta z}{z_0} = -\frac{k^2}{2} - \text{DETERZ} \quad (2b)$$

DETERV and DETERZ are determined from a detailed field theoretical analyses which are described in references [2-9]. In this report we will summarize the results with examples of application to specific substrate and electrode combinations. DETERV and DETERZ depend on the metallization ratio η (Fig. 1) and also on the product of the wavenumber k and the period p of the array. The values are thus different for single-electrodes ($kp = \pi$) and for double-electrodes ($kp = \pi/2$).

As mentioned in the introduction, the v/v_0 and z/z_0 can be ascribed to three different scattering mechanisms: piezoelectric scattering (PS), first-order mechanical scattering (FOMS) and second-order mechanical scattering (SOMS). The overall result may be written as a sum of the three:

$$\frac{\Delta v}{v_0} = p_v \cdot \frac{k^2}{2} + F_v \left(\frac{h}{\lambda}\right) + s_v \cdot \left(\frac{h}{\lambda}\right)^{1.6} \quad (3a)$$

$$\frac{\Delta z}{z_0} = p_z \cdot \frac{k^2}{2} + F_z \left(\frac{h}{\lambda}\right) \quad (3b)$$

where h/λ is the thickness of the electrode in wavelengths. From Equations (3) we may calculate DETERV and DETERZ using Equations (2):

$$\text{DETERV} = -\frac{k^2}{2} (1 + p_v) - F_v \left(\frac{h}{\lambda}\right) - s_v \left(\frac{h}{\lambda}\right)^{1.6} \quad (4a)$$

$$\text{DELTERRZ} = -\frac{k^2}{2} (1 + P_z) - F_z \left(\frac{h}{\lambda}\right) \quad (4b)$$

where the main purpose of this report is to provide means for determining P_v , F_v , β_v , P_z , and F_z . The first term represents the PS component, the second terms the FOMS component and the third the SOMS component. It will be noted that while the first two are given analytically, the last one can only be calculated from a numerical program. The SOMS component, however, only affects DELTERV; it does not affect DELTERZ.

- (1) P_v and P_z are the same for all substrate-electrode combinations and depend only on the metallization ratio. This is true even for buried and bimetal electrodes. This is given in Equations (5) and plotted in Figs. 2 and 3.
- (2) F_v and F_z depend only on the substrate and electrode materials and are independent of the metallization ratio. For a given substrate-electrode combination these may be calculated from Equations (6). The values for chromium and aluminum electrodes on five common substrate orientations are listed in Table III. (Values for intermediate parameters are given in Tables I and II.) Bimetal electrodes are treated in a straightforward manner by adding up the DELTERV and DELTERZ obtained for each metal separately as indicated in Equations 11. For buried electrodes there is no change in $\Delta v/v_0$ but $\Delta z/z_0$ is reduced by $B_S(d/\lambda)$ where d/λ is the groove depth in wavelengths and B_S is a constant, characteristic of the substrate material and orientation -- (see Equation 12 and Table V.) Thus

DELTERZ is modified from Eq. (4b) to

$$\text{DELTERZ} = -\frac{k^2}{2} (1 + P_z) - F_z \left(\frac{h}{\lambda}\right) + B_S \left(\frac{d}{\lambda}\right) \quad (4c)$$

DELTERV remains unmodified from Equation 4a.

- (3) S_v is difficult to express analytically and depends on metallization ratio and the substrate and electrode materials. Moreover, the variation with $(h/\lambda)^{1.6}$ is also approximate. In Fig. 4 the DELTERV for electrodes made of 10% chromium and 90% aluminum is plotted against the total electrode thickness with a metallization ratio $\eta = .5$. This is done for five different substrates and approximate empirical values of S_v are calculated using curve fitting techniques.

B. Piezoelectric scattering

$$P_v = \left\{ -\frac{1}{2\eta} \left[1 + \frac{P_s (-\cos \eta\pi)}{P_{-s} (-\cos \eta\pi)} \right] \right\} \quad (5a)$$

$$P_z = \left\{ -\frac{\pi}{2 \sin \eta\pi} \left[\cos \eta\pi + \frac{P_{-5} (-\cos \eta\pi)}{P_{-0.5} (-\cos \eta\pi)} \right] \right\} \quad (5b)$$

where η is the metallization ratio,

$s = .25$ for double electrodes and

$s = .5$ for single electrodes in Eq. (5a).

P_s is the Legendre function defined by [11]:

$$P_s(x) = \frac{\sin \pi s}{\pi} \sum_{n=0}^{\infty} (-1)^n P_n(x) \left[\frac{1}{s-n} - \frac{1}{s+n+1} \right] \quad (5c)$$

where P_n is the Legendre polynomial of order n . Since there are no reflections from double electrode transducers, $\Delta Z/Z_0$ (Eq. 3b) is provided only for single electrodes.

Figs. 2a and 2b show P_v (for single and double electrodes) and Fig. 3 shows P_z as a function of metallization ratio.

C. First order mechanical scattering

$$F_v = 2\pi \left[|s_1|A_1 + |s_3|A_3 - (|s_1| + |s_2| + |s_3|)A_2 \right] \quad (6a)$$

$$F_z = 2\pi \left[s_1 A_1 + s_3 A_3 + (s_1 + s_2 + s_3) A_2 \right] \quad (6b)$$

s_1, s_2, s_3 represent properties of a freely propagating surface wave:

$$s_1 = -\frac{\omega u_1^2}{4 P_a} \cdot \rho v_o^2 \quad (7a)$$

$$s_2 = -\frac{\omega u_2^2}{4 P_a} \cdot \rho v_o^2 \quad (7b)$$

$$s_3 = -\frac{\omega u_3^2}{4 P_a} \cdot \rho v_o^2 \quad (7c)$$

Here, ω is the radian frequency,

ρ is the mass-density of the substrate,

v_o is the velocity of a freely propagating surface wave,

u_1, u_2, u_3 are the complex particle displacements at the surface for a

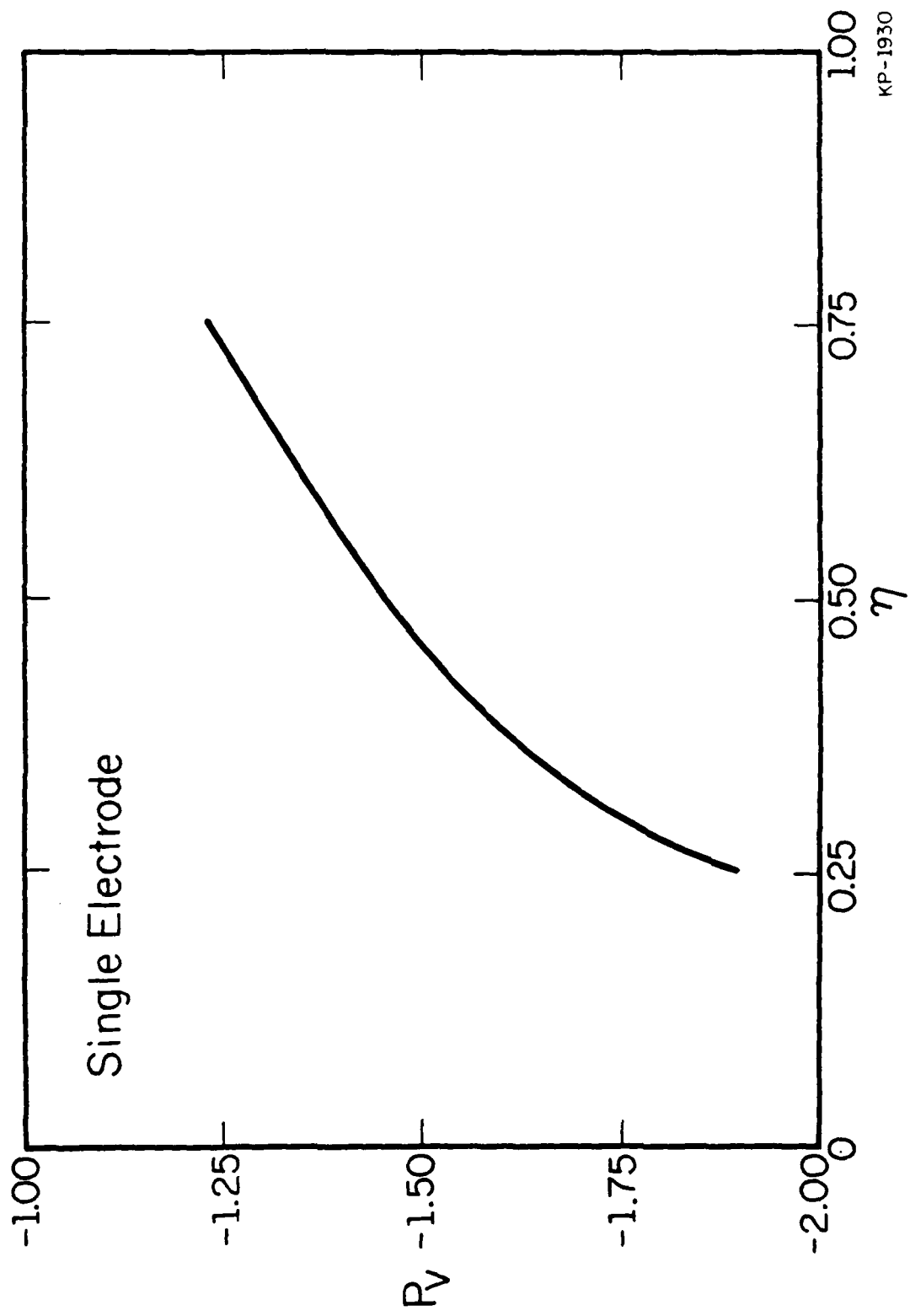


Figure 2a
Piezoelectric scattering coefficient (R_V)
vs duty factor (η) for single electrodes
at $f = v/2p$

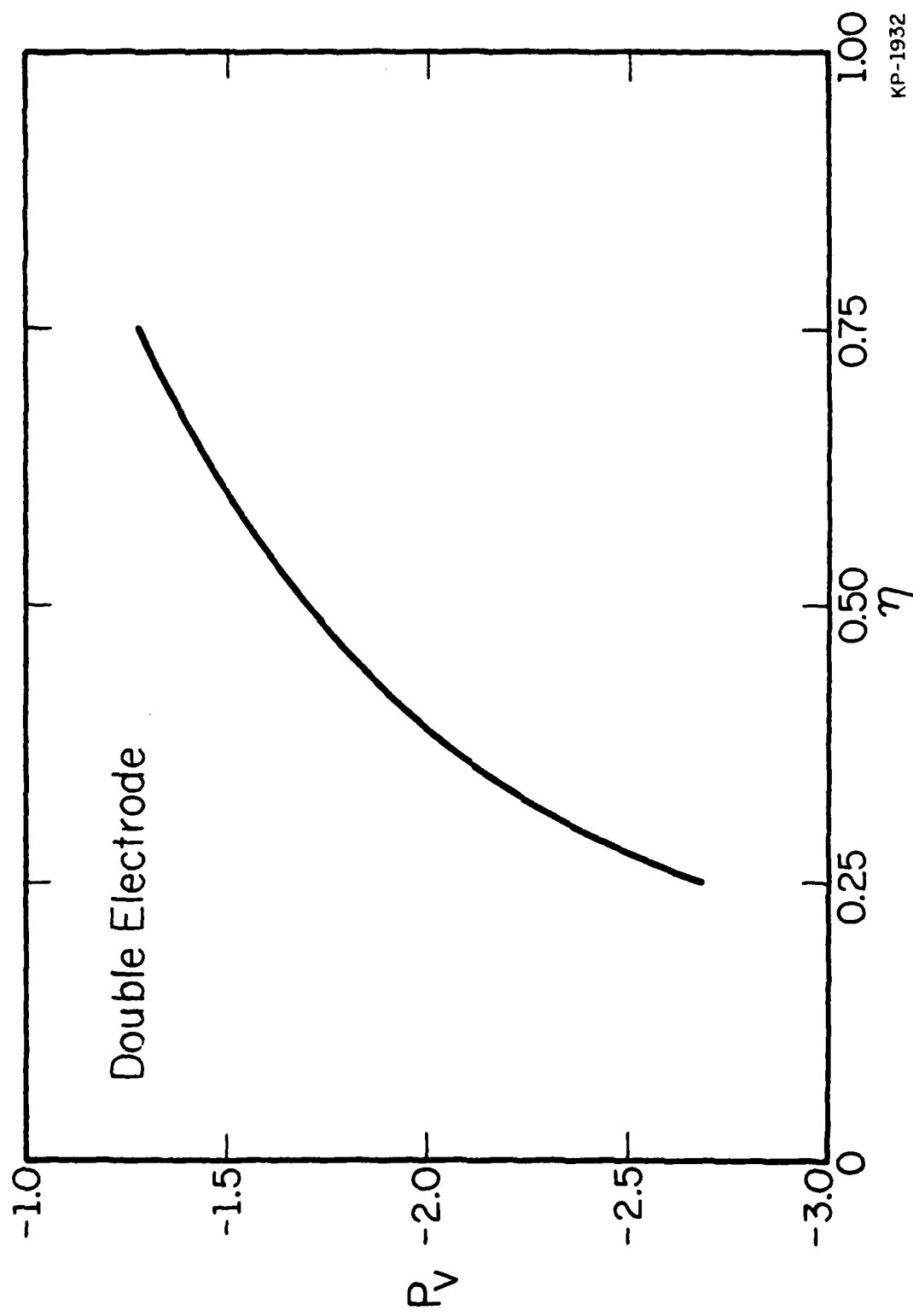


Figure 2b
Piezoelectric scattering coefficient (P_V)
vs duty factor (η) for double electrodes
at $f = v/4p$

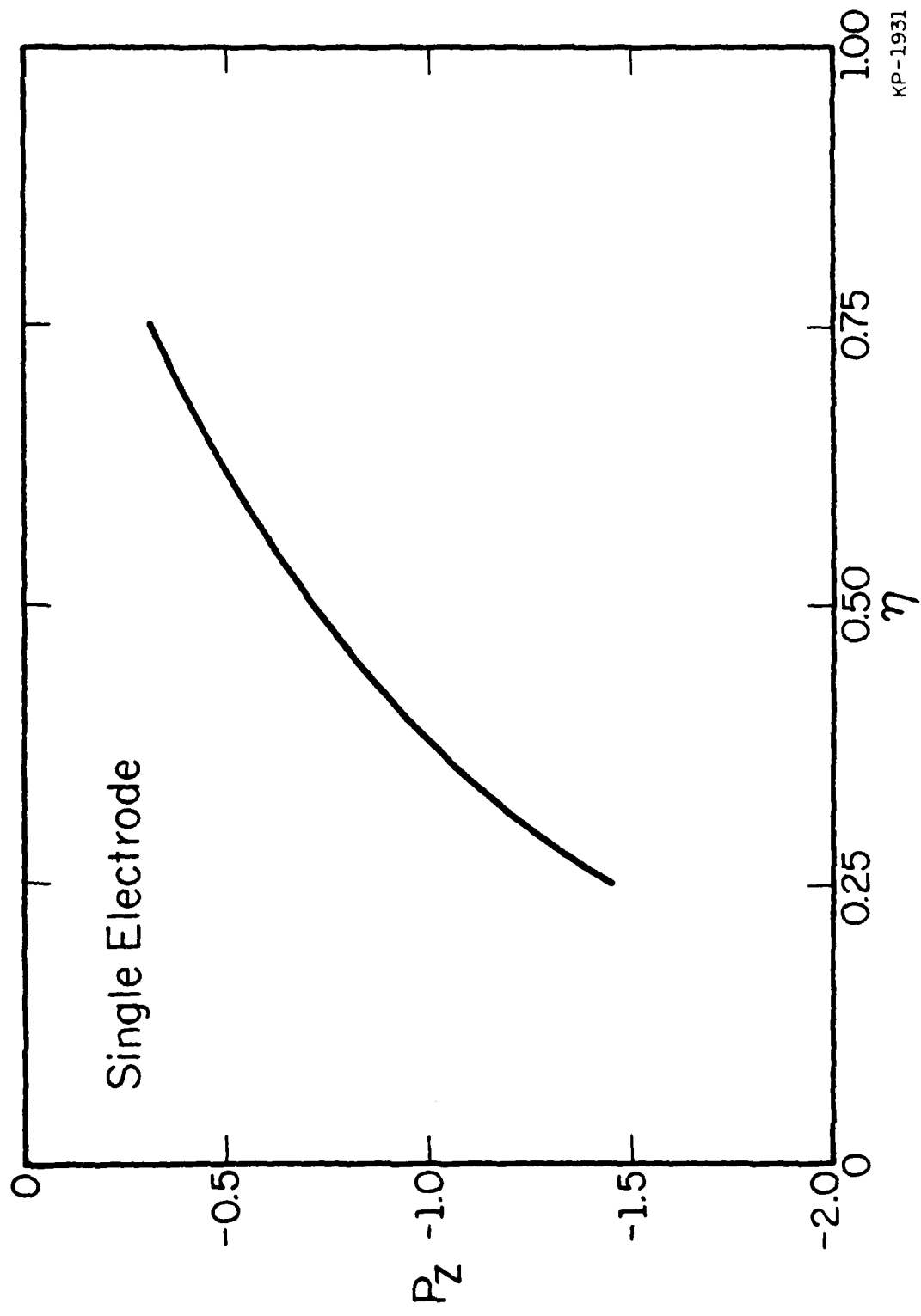


Figure 3
Piezoelectric scattering factor P_z vs
duty factor (η) for single electrodes
at $f = v/2p$

surface wave carrying a power P_n per unit beamwidth. The phases of u_1 , u_2 , u_3 should be with reference to the surface potential. It will be noted that S_1 , S_2 , S_3 as defined above are dimensionless numbers independent of frequency. Their values are tabulated below for 5 common substrate orientations. These can be computed from the data in the microwave acoustics handbook, Vol. 1A [15].

TABLE I
Substrate Parameters

<u>Substrate</u>	ρ (kg/m ³)	v_o (m/sec)	$K^2/2$	$\rho v_o^2 (10^{10} \text{ nt/m}^2)$	S_1	S_2	S_3
ST Quartz ¹⁶	2651	3159	.000275	2.65	-.001	-.12	.052
YZ LiNbO ₃	4700	3490	.0246	5.72	0	-.096	.044
37.95, X LiNbO ₃ ¹⁷	4700	3996	.030	7.50	-.0006	-.166	.135
MDC LiTaO ₃ ¹⁸	7450	3379	.0077	8.51	0	-.164	.124
100 cut 110 prop. GaAs	5307	2864	$\approx .00027$	4.35	0	-.185	.103

The other parameters in Equations (5) A_1 , A_2 , A_3 are also dimensionless and represent the material properties of the electrode material normalized to the substrate:

$$A_1 = \alpha'_1 / \rho v_o^2 \quad (8a)$$

$$A_2 = \rho' / \rho \quad (8b)$$

$$A_3 = \alpha'_3 / \rho v_o^2$$

Here α'_1 , ρ' , α'_3 represent material properties of the electrode (the prime is

used to distinguish these from the substrate properties). ρ' is the mass-density of the electrode while α'_1 , α'_3 are effective stiffness coefficients. If the electrode is isotropic (which is commonly true),

$$\alpha'_1 = \mu \quad (9a)$$

$$\alpha'_3 = \frac{4\mu(\lambda + \mu)}{\lambda + 2\mu} \quad (9b)$$

where λ and μ are the Lamé constants. For anisotropic materials we have,

$$\alpha'_1 = \frac{s'_3}{D} \quad (10a)$$

$$\alpha'_3 = \frac{s'_5}{D} \quad (10b)$$

$$\text{where } s'_I^J = \frac{s'_{11}s'_{IJ} - s'_{IJ}s'_{11}}{s'_{11}}$$

$$\text{and } D = s_5^{53} - s_3^{53}$$

with s'_{IJ} representing the compliance tensor for the electrode material in the abbreviated subscript notation. α'_1 and α'_3 are tabulated below for a few common electrode materials:

TABLE II
Metal Parameters

<u>Electrode</u>	$\rho' (\text{kg/m}^3)$	$\alpha_1' (10^{10} \text{nt/m}^2)$	$\alpha_3' (10^{10} \text{nt/m}^2)$
Chrome	7200	10.0	28.24
Aluminum	2695	2.5	7.75
Gold	19300	2.85	9.83
Silver	10490	2.7	8.71
Titanium	4500	4.4	12.93

Using Tables I and II, DELTERV and DELTERZ can be calculated from Equations (4) for any electrode-substrate combination. Note that F_v and F_z are constants for a particular substrate-electrode combination independent of the metallization ratio. For convenience, these are tabulated below for the five electrodes listed in Table II on the five substrates listed in Table I.

TABLE III
First Order Mechanical Scattering Constants F_V , F_Z

<u>Electrode:</u>	<u>Chromium</u>		<u>Aluminum</u>		<u>Gold</u>		<u>Silver</u>		<u>Titanium</u>	
<u>Substrate</u>	F_V	F_Z	F_V	F_Z	F_V	F_Z	F_V	F_Z	F_V	F_Z
ST Quartz	.55	+2.28	-.15	+.51	-6.64	-1.95	-3.22	-.65	-.24	+.85
YZ LiNbO ₃	.02	+.87	-.13	+.19	-3.14	-.87	-1.63	-.34	-.22	+.31
37.95,X LiNbO ₃	.3	+2.89	-.21	+.76	-6.69	-.29	-3.2	+.54	-.35	+1.27
MDC LiTaO ₃	.83	+2.34	+.06	+.62	-3.79	+.25	-1.75	+.44	+.092	+1.033
100 cut 110 prop. GaAs	+1.74	+3.5	+.23	+.89	-5.1	-.42	-2.23	+.28	+.389	+1.486

D. Second order mechanical scattering

Unfortunately the results of this part of the problem could not be reduced to analytic form and have to be obtained from a numerical program. We have chosen a typical bimetal electrode with 10% chromium and 90% aluminum and plotted DELTERV against h/λ (h being the total electrode thickness) for five different substrates, assuming a metallization ratio $\eta = .5$. In Figures 4 and 5 we have indicated values of S_V that best fit the curve in accordance with Equation (3a). A convenient summary is provided in Table IV.

It will be noted that this effect is a higher power in h/λ so that for sufficiently thin electrodes it may be neglected in comparison to the other effects.

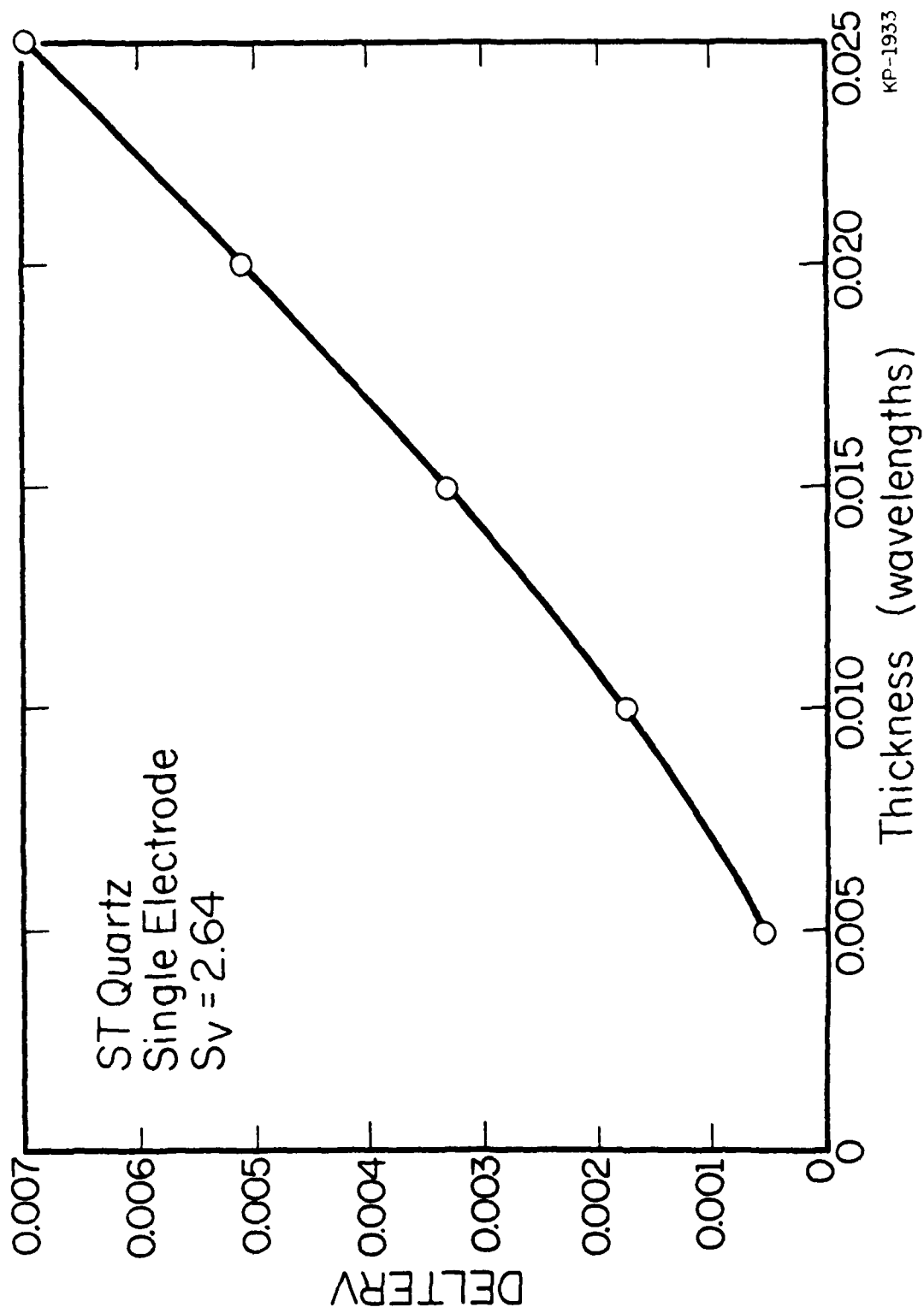


Figure 4a

SOMS DELTERV vs electrode thickness
single electrode ST QUARTZ
 $S_V = 2.64 \ (h/\lambda)^{1.6}$

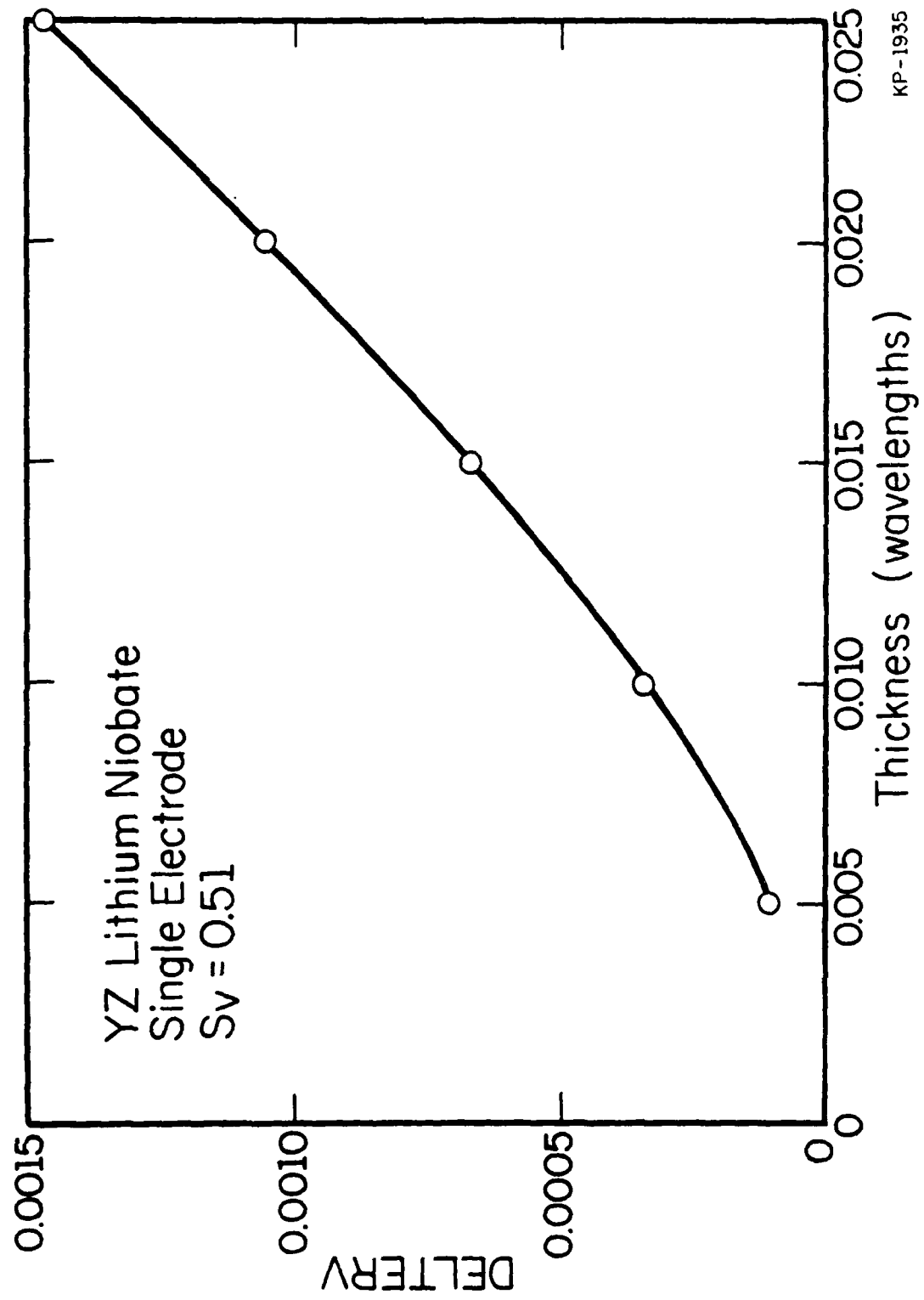


Figure 4b

SOMS DELTERV vs electrode thickness
single electrode YZ LiNbO₃
SOMS DELTERV = 0.51 $(h/\lambda)^{1.6}$

20

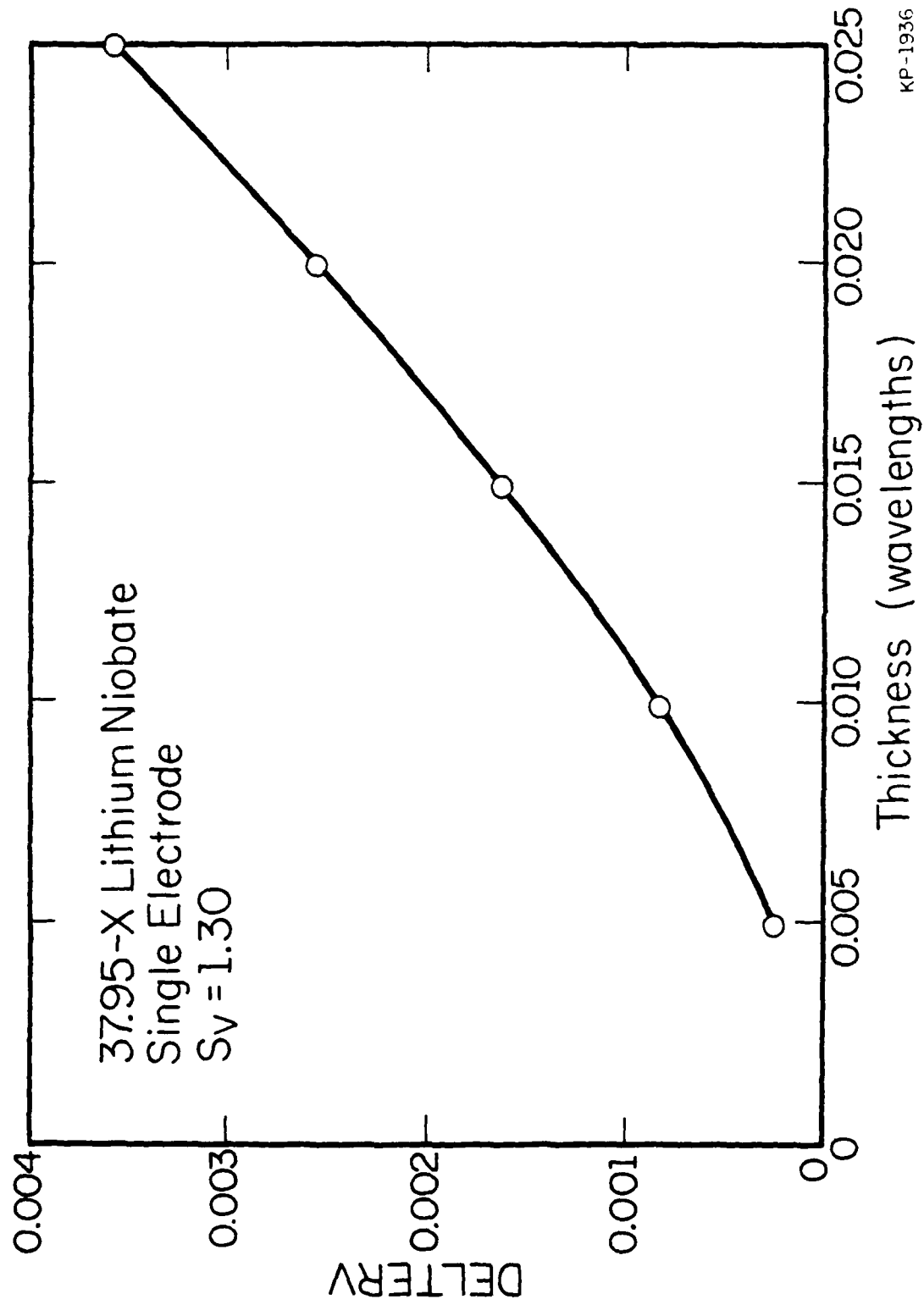


Figure 4c

SOMS DELTERV vs electrode thickness
single electrode 37.95-X LiNbO₃
SOMS DELTERV = 1.30 (h/λ) 1.6

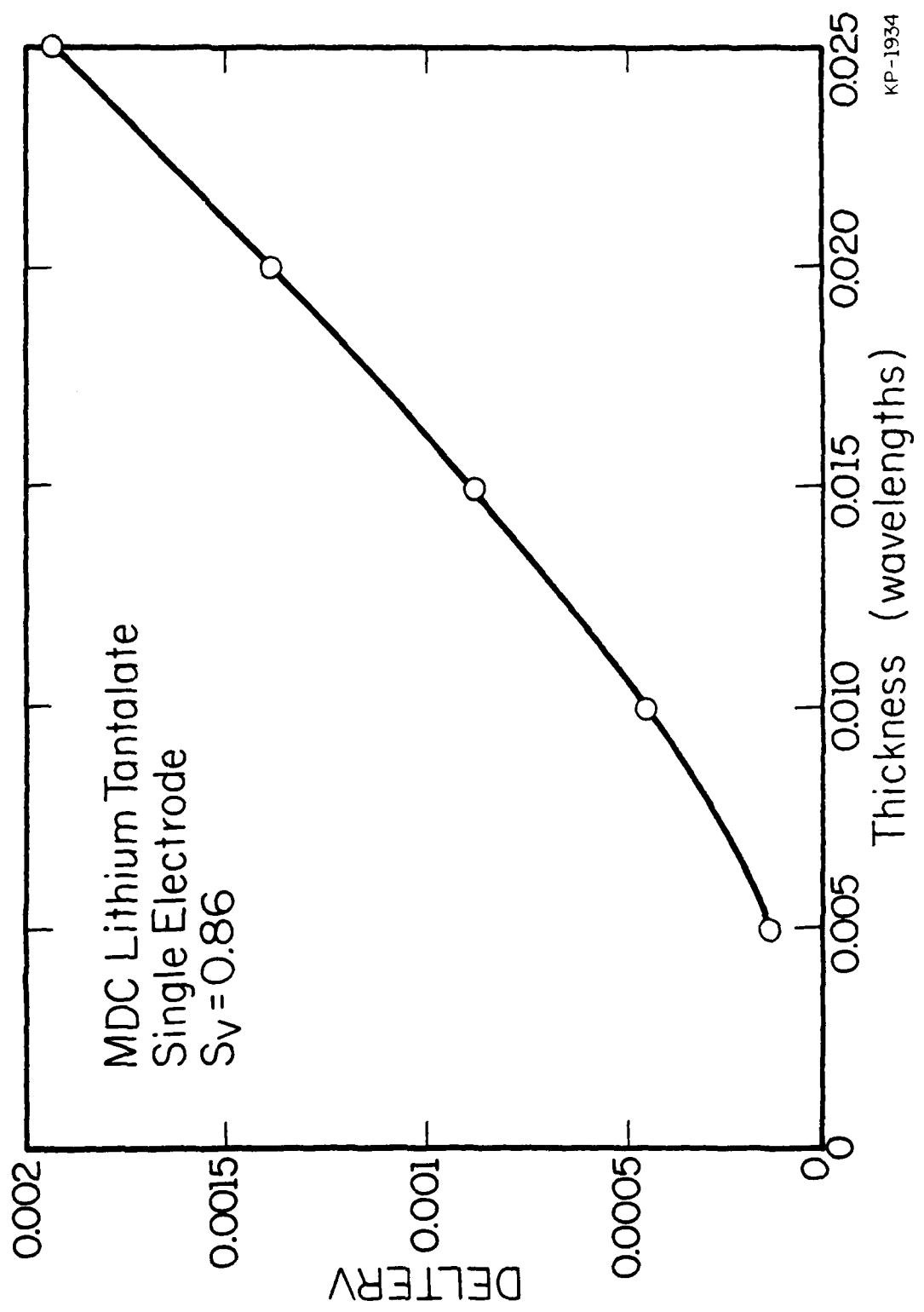


Figure 4d

SOMS DELTERV vs electrode thickness

single electrode MDC LiTaO₃SOMS DELTERV = 0.86 $(\hbar/\lambda)^{1.6}$

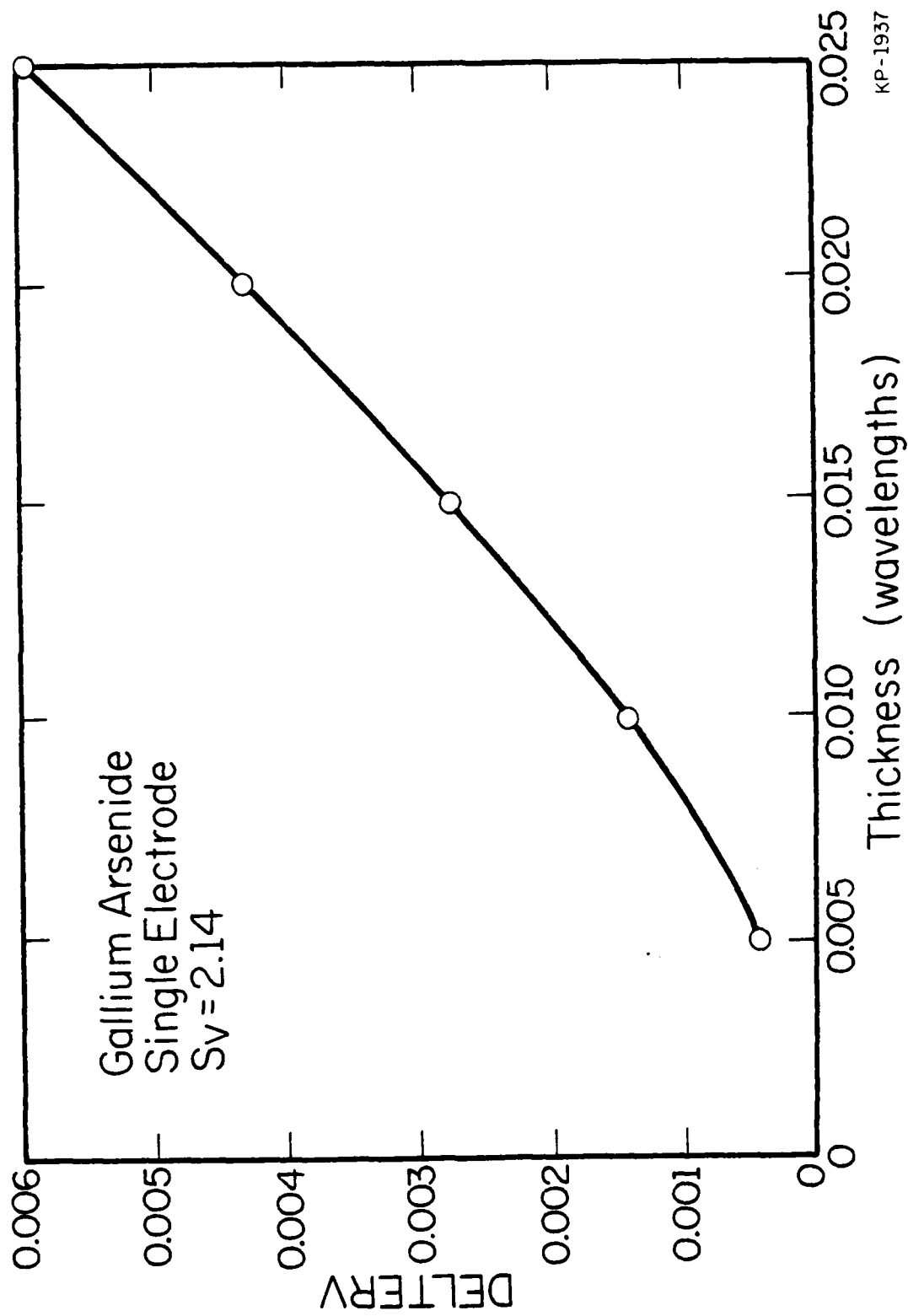


Figure 4e

SOMS DELTERV vs electrode thickness
single electrode GaAs
SOMS DELTERV = $2.14 (h/\lambda)^{1.6}$

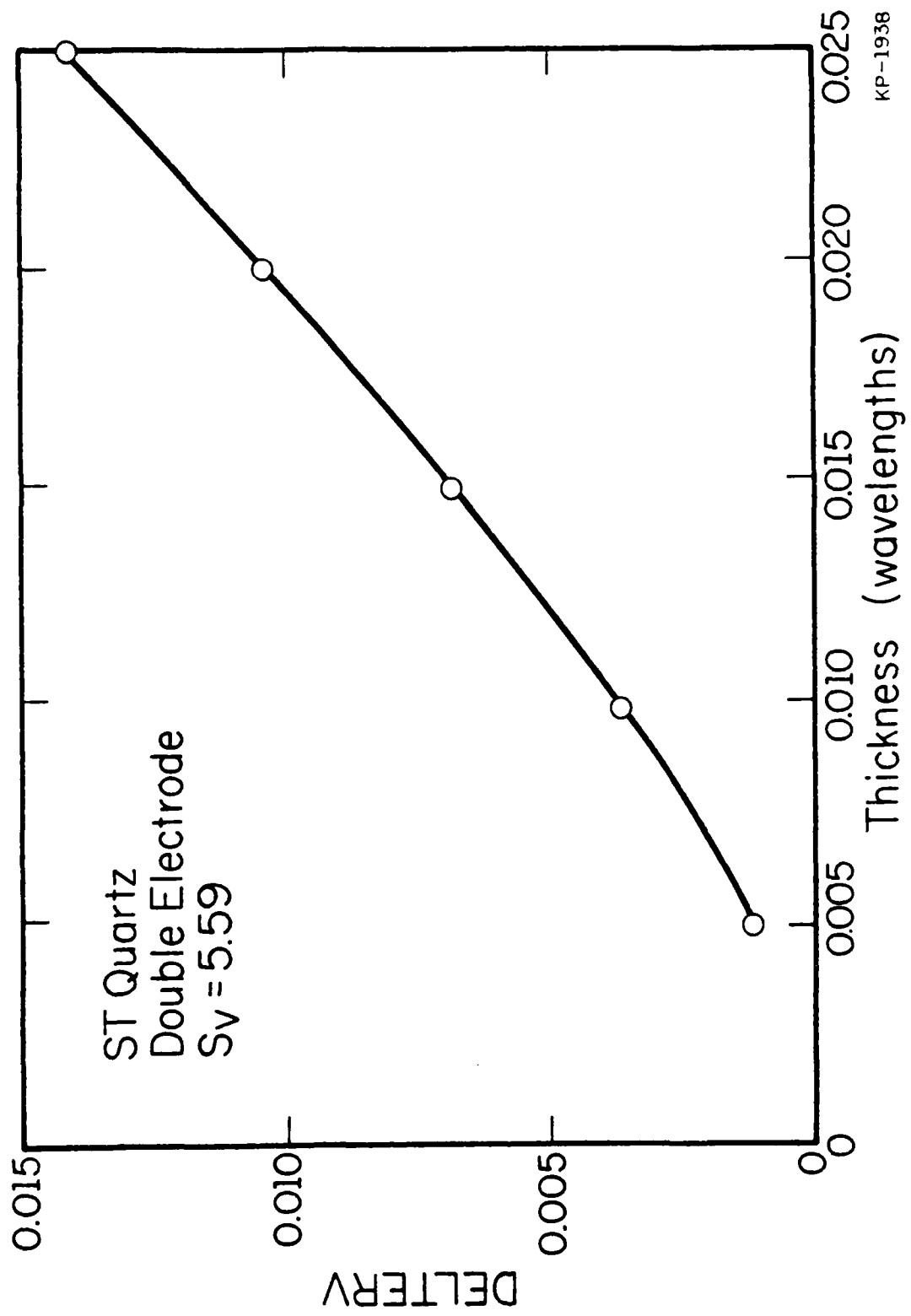


Figure 5a
SOMS DELTERV vs electrode thickness
double electrode ST QUARTZ
 $S_{OMS} \text{ DELTERV} = 5.59 (h/\lambda)^{1.6}$

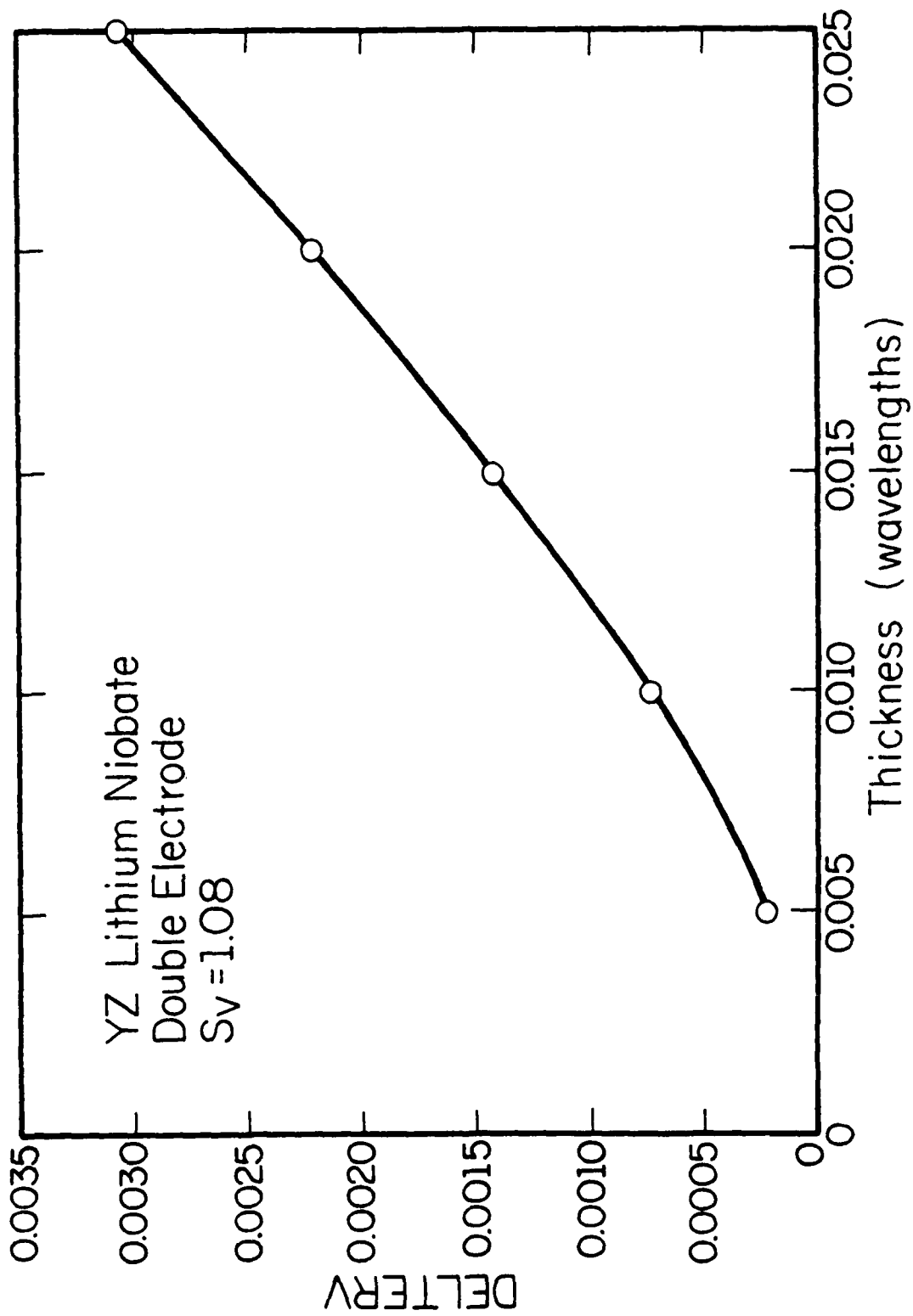


Figure 5b
SOMS DELTERV vs electrode thickness
double electrode YZ LiNbO₃
SOMS DELTERV = $1.08 (\lambda/\text{nm})^{1.6}$

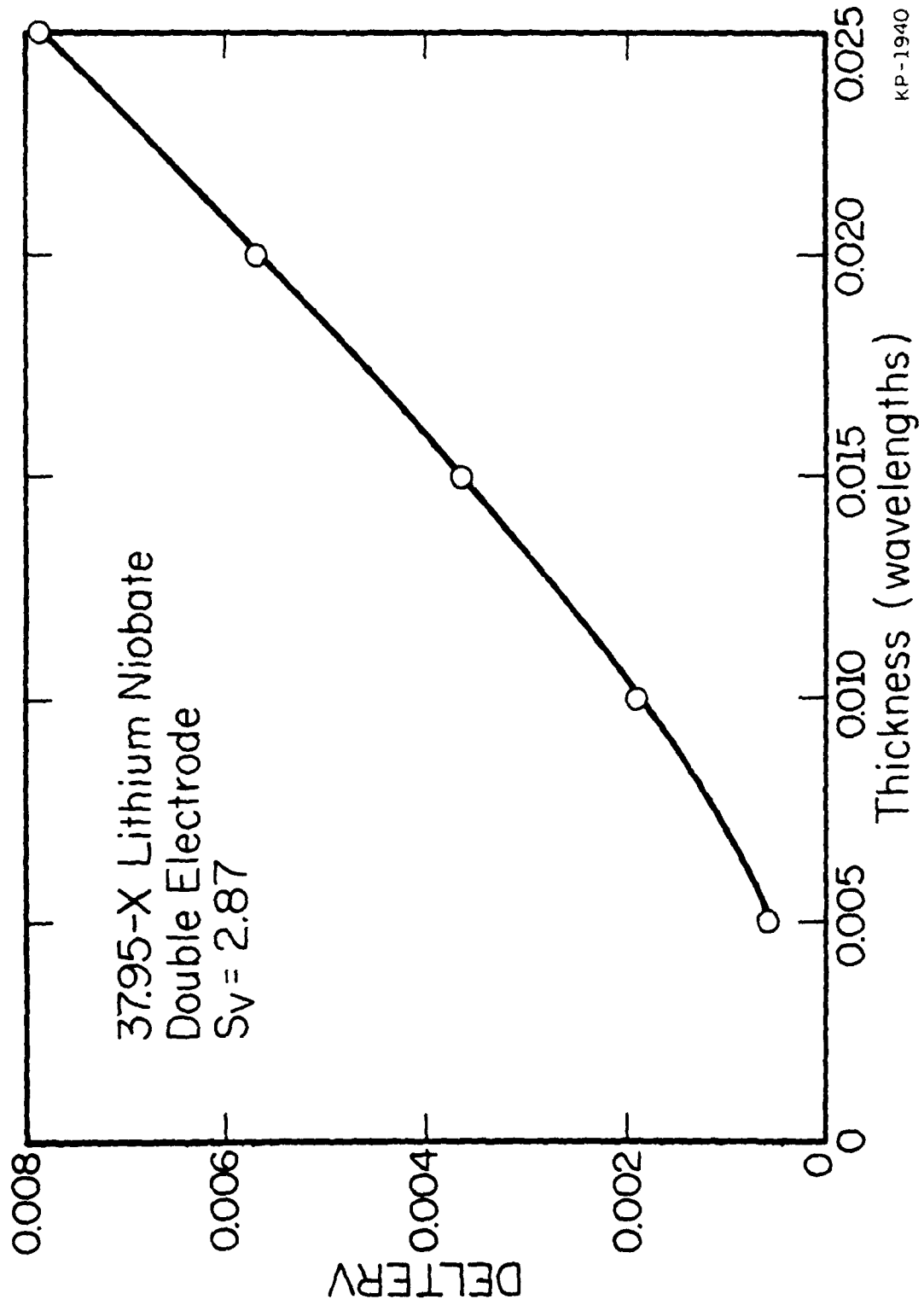


Figure 5c
SQUID DELTERV vs electrode thickness
double electrode 37.95-X LiNbO₃
SQUID DELTERV = $2.87 (h/\lambda)^{1.6}$

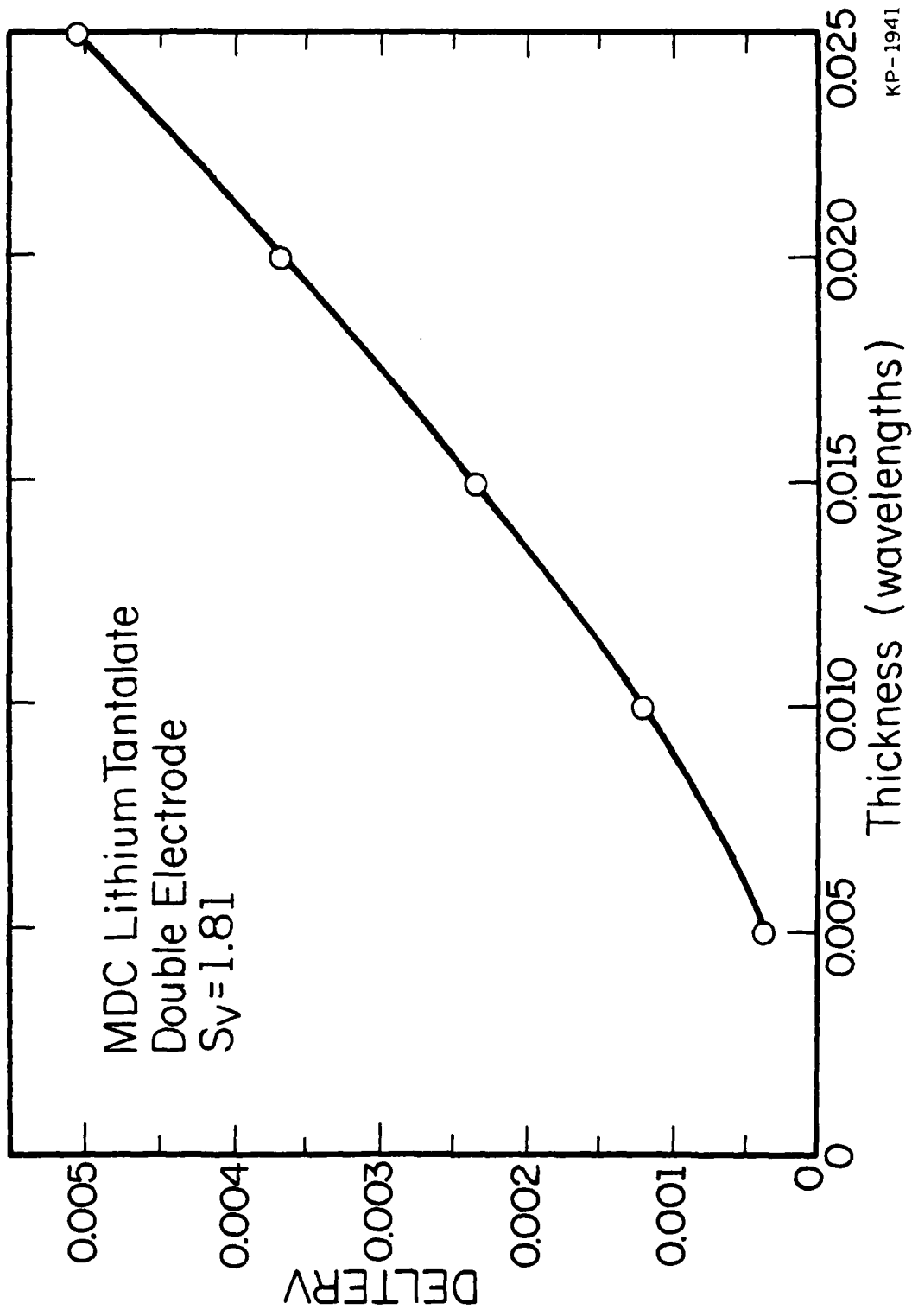


Figure 5d

SOWS DELTERV vs electrode thickness
double electrode MDC LiTaO₃
SOWS DELTERV = 1.81 $(h/\lambda)^{1.6}$

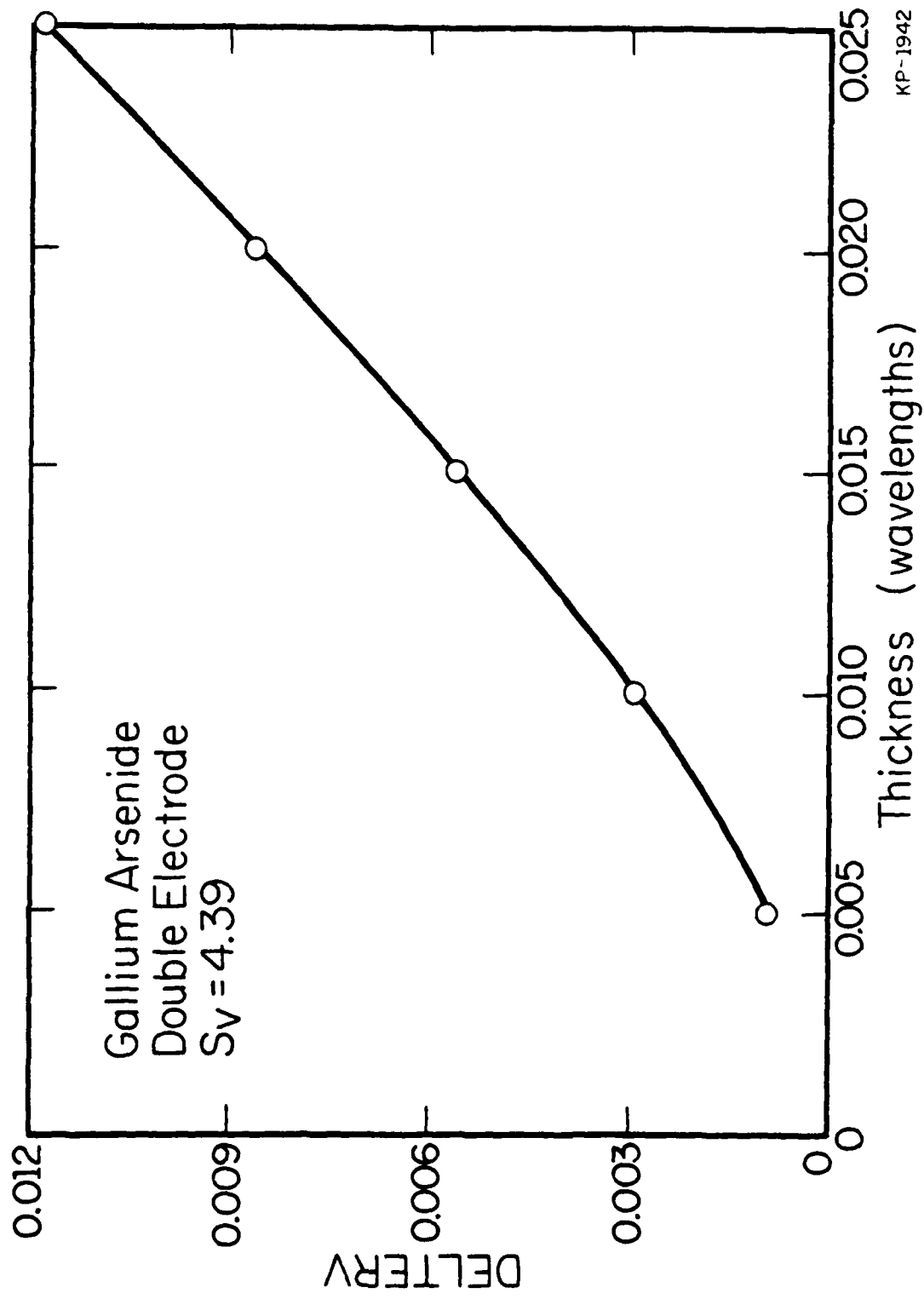


Figure 5e
SOMS DELTERV vs electrode thickness
double electrode GaAs
SOMS DELTERV = $4.39 (h/\lambda)^{1.6}$

TABLE IV

Second Order Mechanical Scattering Coefficient S_V
of 10% Cr 90% Al: 5 substrates

	S_V Single Electrode	S_V Double Electrode
ST Quartz	-2.64	-5.59
YZ LiNbO ₃	-.51	-1.08
37.95,X LiNbO ₃	-1.3	-2.87
MDC LiTaO ₃	-0.86	-1.81
100 cut, 110 prop. GaAs	-2.14	-4.34

It will be noted from Eq.(4a) that a negative S_V means a positive DELTERV which corresponds to a slowing of the wave. The stored energy effect always slows down the wave.

E. Additional discussion on bimetal electrodes

The FOMS and SOMS coefficients change as the composition of bimetal electrodes are altered. The SOMS must be recomputed for each bimetal composition, but in many cases the electrodes are sufficiently thin so that the SOMS component is negligible. The FOMS coefficients for bimetal electrodes are determined by averaging the F_V and F_Z for the individual metals and using total electrode thickness. For example, if an electrode is made of chromium of height h_1 and aluminum of height h_2 and the substrate is ST-cut quartz, then:

$$\begin{aligned}
 \bar{F}_V &= F_{V1} \frac{h_1}{h_1+h_2} + F_{V2} \frac{h_2}{h_1+h_2} \\
 &= .55 \frac{h_1}{h_1+h_2} - .15 \frac{h_2}{h_1+h_2}
 \end{aligned} \tag{11a}$$

$$\begin{aligned}
 \bar{F}_Z &= F_{Z1} \frac{h_1}{h_1+h_2} + F_{Z2} \frac{h_2}{h_1+h_2} \\
 &= 2.28 \frac{h_1}{h_1+h_2} + .51 \frac{h_2}{h_1+h_2}
 \end{aligned} \tag{11b}$$

where:

F_Z , \bar{F}_Z are the average FOMS constants

F_{Z1} , F_{V1} are the FOMS constant for metal 1

F_{Z2} , F_{V2} are the FOMS constant for metal 2

h_1 is the thickness of metal 1

h_2 is the thickness of metal 2

An electrode made of 10% Cr and 90% Al has an effective $F_V = -.08$
 $(=.55 \times .1 - .15 \times .9)$ and $F_Z = .69$ ($= 2.28 \times .1 + .51 \times .9$).

F. Buried electrodes

The FOMS and SOMS are both affected when an electrode is buried. The SOMS must be recomputed using the numerical program but it only affects the velocity shift and does not alter the impedance mismatch. Since electrodes

are buried to reduce reflections, the FOMS is the important parameter. The FOMS for buried electrodes are calculated by viewing the gap regions as being made up of electrodes of the same material as the substrate. The velocity, v_0 in the gap regions remains the same as before; however, the impedance changes somewhat. For example, a grooved array reflector can be viewed as an array with electrodes made of the substrate material. In such an array the first-order SAW velocity is the same as on a free substrate implying zero v/v . However, it produces reflections implying a non-zero Z/Z_0 . A buried electrode array may be viewed as a normal electrode array interleaved with a grooved array. The Z/Z_0 is reduced by a quantity proportional to the depth of the grooves (thickness of the electrode made of substrate material).

$$\frac{\Delta Z}{Z_0} \Big|_{\substack{\text{buried} \\ \text{electrode}}} = \frac{\Delta Z}{Z_0} \Big|_{\substack{\text{non-buried} \\ \text{electrode}}} - B_S \cdot \left(\frac{d}{\lambda}\right) \quad (12a)$$

where d/λ is the depth of the groove in wavelengths, and B_S is a constant depending on the substrate and is given by equation (12b), which is similar to Equation (6b).

$$B_S = 2\pi \left[S_1 A_1 + S_3 A_3 + (S_1 + S_2 + S_3) \right] \quad (12b)$$

The DELTERZ for buried electrodes has been indicated earlier in Equation (4c). S_1 , S_2 , S_3 are defined as in Equations (7) and are listed for five different substrates in Table I. A_1 and A_3 are defined as in Equation (9):

$$A_1 = \alpha'_1 / \rho v_o^2 \quad (13a)$$

$$A_3 = \alpha'_3 / \rho v_o^2 \quad (13b)$$

However, α'_1 and α'_3 are given by Equations (10) rather than Equations (9) because substrates are usually anisotropic in contrast to the electrodes. In Equations (10), s' now represents the compliance tensor for the substrate material and not that for the electrode material.

A_1 and A_3 for the five substrates are listed in Table V.

TABLE V
Substrate Constants Pertinent to the Non-Electrode Sections
of a Buried Electrode Case

<u>Substrate</u>	A_1	A_3
ST Quartz	2.51	3.28
YZ-LiNbO ₃	0	3.66
37.95, X LiNbO ₃	1.03	2.48
MDC LiTaO ₃	1.26	2.63
100 cut, 110 prop. GaAs	2.3	6.49

Table VI shows B_s calculated from Equation 12 for the five substrates:

TABLE VI

 B_S for Different Substrates

<u>Substrates</u>	B_S
ST Quartz	.62
YZ-LiNbO ₃	.69
37.95, X LiNbO ₃	1.9
MDC LiTaO ₃	1.19
100 cut, 110 prop. GaAs	-.03

Section III: Finite Array Analysis

A. Physical Interpretation of Neighboring Electrode Effects

The scattering properties of one electrode in an array depend on the electrodes that precede and follow it. The infinite array analyses presented in the previous section assume that all preceding and following electrodes are in place and identical to the electrode in question. In this section the scattering properties of the electrodes at the end of the finite array are examined. The piezoelectric scattering, the first order mechanical scattering and the second order mechanical "stored energy" scattering are all affected differently. In each case a correction factor which converts the infinite array DELTERZ and DELTERV to the finite array is determined.

Both the single and double electrode structures are analyzed at their respective synchronous frequencies. In each case, one, two, three, four and N electrode arrays are considered. A finite array factor which relates the finite array DELTERV and DELTERZ to the infinite array counterparts is calculated for each case.

The following three sections discuss how the finite array factor is calculated for each type of scattering and the final section summarizes the results and provides the equations and values required to calculate the transmission line parameters.

1. Piezoelectric Scattering

The variation of the electric to acoustic coupling strength of transducer electrodes depends on the existence and shape of neighboring electrodes. Szabo et al. [10] and Smith et al. [11] have determined the effective strength of electrodes in an ordinary withdrawal weighted transducer. Lentine et al. [8] extended this analysis to a withdrawal weighted transducer with arbitrary voltages on the electrodes. These analyses are correct for transducer coupling strength but do not predict the nearest neighbor dependence in velocity shift or acoustic impedance mismatch.

The DELTERZ and DELTERV of the end electrodes in a finite array are determined by using the infinite array electrical loading analysis from the previous section in conjunction with Lentine's withdrawal weighted transducer analysis. The analysis is described in a thesis by Lentine [12] and in the Appendix and implements the following approach:

- * The charge is calculated for each electrode in an infinite array.
- * A fictitious transducer is designed so that the taps which represent the existing electrodes in the finite array have zero voltage and the taps which represent the missing electrodes beyond the end of the finite array have a charge distribution equal to and opposite that of an infinite array electrode. This transducer is synthesized using the withdrawal weighted transducer theory of Lentine [7].
- * The transducer solution is added to that of the infinite array and the result is a solution that satisfies the boundary conditions for a finite array, namely, zero volts on the existing electrodes and zero charge on the surface where electrodes have been removed to form a

finite array.

- * The charge of each electrode in the finite array is then known and DELTERV and DELTERZ are calculated using the same technique as used in the infinite array case.

2. First Order Mechanical Scattering of Finite Arrays

The velocity shift and impedance mismatch caused by first order elastic loading has no nearest neighbor dependence because the substrate is assumed rigid with substrate distortion accounted for in the stored energy analysis. Since the substrate is rigid, there is no elastic coupling from one electrode to another and the infinite array first order elastic loading analysis is valid for finite arrays as well.

3. Second Order Mechanical Scattering in Finite Arrays

The velocity shift and acoustic impedance mismatch arising from stored energy effects is somewhat dependent on neighboring electrodes. When a wave passes under an electrode, the metal exerts a mechanical force on the surface. This force generates forward and reverse waves which are accounted for in the first order analysis and it produces evanescent distortions which do not propagate away. The internal forces arising from the localized substrate distortions work against the particle velocity of the incident wave to generate forward and reverse traveling waves over and above those accounted for in the first order analysis. The reverse waves, known as reflections, are accounted for by DELTERZ and the forward waves, known as velocity shifts, are accounted for by DELTERV. These parameters are therefore directly related to the substrate distortion under the electrode in question. The localized distortion produced by an electrode extends some distance in each direction.

When the distortions of one electrode overlaps with another, nearest neighbor effects arise. One would therefore expect that DELTERV and DELTERZ for the end electrode of a finite array would differ somewhat from that of one in an infinite array.

The infinite array stored energy program has been modified to calculate the difference in DELTERV and DELTERZ produced by removing the first nearest neighbor. Fortunately the nearest neighbor stored energy effects are small. The Appendix shows by example that the stored energy effect is only slightly perturbed (~ 5 - 10%) by the absence of adjacent electrodes. This is in contrast to piezoelectric scattering which is strongly affected by the neighboring electrode configuration. There is also experimental evidence that the stored energy velocity shifts are independent of nearest neighbors. The infinite array value of DELTERV for chrome-Al electrodes on ST quartz when used in a second order effects transducer analysis program [16] provides a response very similar to that measured experimentally at RADC for withdrawal weighted transducers. The withdrawal weighted transducer presents a very stringent test of nearest neighbor dependence and this indicates that the infinite array values of SOMS are sufficiently accurate for use in finite array analysis. By contrast, on strongly piezoelectric substrates like LiNbO₃, when the infinite array values of DELTERV were used in the analysis program for a withdrawal weighted transducer, the response did not agree with the RADC experimental response. This is expected since the piezoelectric scattering is significantly neighbor dependent.

B. Finite Array Parameters Defined in Terms of Infinite Array Results

The finite array factors relate each component of the finite array transmission line parameter to its infinite array counterpart. The finite array factors are calculated using the analysis described in the last section and are tabulated in Table VII. The finite array transmission line parameters are calculated using values in Table VII, the infinite array parameters and equations 14.

$$DV_{ijk} = - \left(1 + \alpha_{V_{ijk}} \cdot p_V \right) \frac{k^2}{2} - F_V\left(\frac{h}{\lambda}\right) - S_V\left(\frac{h}{\lambda}\right)^{1.6} \quad (14a)$$

$$DZ_{ijk} = - \left(1 + \alpha_{Z_{ijk}} \cdot p_Z \right) \frac{k^2}{2} - F_Z\left(\frac{h}{\lambda}\right) \quad (14b)$$

DV_{ijk} is the DELTERV of the jth electrode counted from the nearest end of a "k" electrode finite array

DZ_{ijk} is the DELTERZ of the jth electrode counted from the nearest end of a "k" electrode finite array

i is "S" for single electrode and "D" for double electrodes

$\alpha_{V_{ijk}}$ is the finite array factor that relates the infinite array scattering to the finite array DELTERV component specified by "i", "j", and "k"

$\alpha_{Z_{ijk}}$ is the finite array factor that relates the infinite array scattering to the finite array DELTERZ component specified by "i", "j", and "k"

Most of the finite array factors are close to "one", the only exception being $\alpha_{Z_{S11}}$. A finite array factor equal to "one" arises when the infinite array parameter is equal to the finite array value. The finite array factors of this table in conjunction with Equations 14 and infinite array parameters allow the calculation of the transmission line parameters for any length of finite array.

TABLE VII
Finite Array Factors for Piezoelectric Scattering

(a) $\alpha_{V_{Sjk}}$ for single electrodes

	k:	1	2	3	4	5
j:	1	.73	.88	.86	.86	.86
2	X		.88	1.05	1.02	1.02
3	X	X		.86	1.02	1.02

(b) $\alpha_{Z_{Sjk}}$ for single electrodes

	k:	1	2	3	4	5
j:	1	.16	.63	.56	.57	.57
2	X		.63	1.13	1.05	1.05
3	X	X		.56	1.05	1.05

(c) $\alpha_{V_{Djk}}$ for double electrodes

	k:	1	2	3	4	5
j:	1	.91	.94	.95	.95	.95
2	X		.94	1.02	1.02	1.02
3	X	X		.95	1.02	1.02

k is the number of electrodes in the finite array

j is the electrode number counted from the nearest end

Section IV: Low Perturbation Bimetal Electrodes

A. Cancellation of Piezoelectric Scattering by Mechanical Scattering

Electrodes placed on the surface for the purpose of generating and detecting surface acoustic waves will inevitably produce a piezoelectrically induced velocity shift and impedance mismatch. It is the purpose of this section to suggest a bimetal electrode in which the mechanically induced velocity shift or impedance mismatch precisely cancels the piezoelectric perturbations. The results have not been experimentally verified. It is shown that either velocity shift or impedance mismatch can be eliminated but not both. It is not possible to find an electrode that eliminates both simultaneously.

Consider first the shift in velocity produced by the electrode as described in Section II. The PS and the SOMS always slow the wave, while the FOMS may either speed or slow the wave depending on the electrode and substrate materials. The zero velocity shift and zero impedance mismatch condition derived from equations 4 - 11 are:

FOMS PS SOMS

$$\bar{F}_V \frac{h}{\lambda} = - \frac{k^2}{2} P_V - S_V \left(\frac{h}{\lambda} \right)^{1.6} \quad (15a)$$

$$\bar{F}_Z \frac{h}{\lambda} = - \frac{k^2}{2} P_Z \quad (15b)$$

Solving for \bar{F}_V and \bar{F}_Z :

$$\bar{F}_V = -\frac{k^2}{2} \frac{P_V}{h/\lambda} - S_V(h/\lambda)^{.6} \quad (16a)$$

$$\bar{F}_Z = -\frac{k^2}{2} \frac{P_Z}{h/\lambda} \quad (16b)$$

The PS and SOMS both slow the wave and produce a negative impedance mismatch. The best way to suppress the SOMS effects is to use thin electrodes. The perturbation cancelling approach will not work well with thick electrodes where SOMS is significant. In thick electrodes, a large FOMS is used to cancel a similarly large PS and SOMS component. Even if the fabrication process could be controlled precisely to make the subtraction of two large numbers produce a zero velocity shift, the impedance mismatch would be large. If the thick electrodes are designed to null the impedance mismatch, the velocity shift will be large.

The thin electrode conditions for zero velocity shift and impedance mismatch are:

$$\bar{F}_V = -\frac{k^2}{2} \frac{P_V}{h/\lambda} \quad \frac{h}{\lambda} \ll \left| \frac{k^2}{2} \frac{P_V}{S_V} \right|^{1.6} \quad (17a)$$

$$\bar{F}_Z = -\frac{k^2}{2} \frac{P_Z}{h/\lambda} \quad (17b)$$

This is a rather severe requirement for weak coupling materials such as ST Quartz where $h/\lambda \ll .004$. It is less stringent for stronger coupling coefficient materials such as LiNbO_3 .

Simultaneous cancellation of velocity shift and impedance mismatch requires that

$$F_Z = (P_Z/P_Y)F_Y$$

This condition cannot be met because F_Z is always larger than F_Y (see Eq. 6) and $|P_Y|$ is always greater than $|P_Z|$ (see Figs. 4,5). Therefore, the rest of this section is dedicated to finding a bimetal electrode in which the impedance mismatch is nulled for single electrodes where reflections are a serious problem and velocity shift is nulled for double electrodes where electrode symmetry suppresses the reflections.

B. Low Impedance Mismatch for Single Electrodes

The impedance mismatch of a bimetal single electrode in an infinite array is cancelled if the average \bar{F}_Z is positive and has the value:

$$\bar{F}_Z = -P_Z \frac{K^2}{2} \frac{1}{(h/\lambda)} \quad (19a)$$

$$P_Z = -.75 \quad \text{at} \quad \eta = .5 \quad (\text{Fig. 4}) \quad (19b)$$

$$\bar{F}_Z = \frac{.375 K^2}{h/\lambda} \quad (19c)$$

The \bar{F}_Z required for impedance mismatch cancellation are tabulated for five substrates and three typical electrode thicknesses in Table VIII.

TABLE VIII
 \bar{F}_Z required for zero SE impedance mismatch

	Electrode Thickness		
	$h/\lambda = .001$	$h/\lambda = .01$	$h/\lambda = .025$
ST Quartz	.2	X	X
YZ LiNbO ₃	18.5	1.85	0.75
37.95,X LiNbO ₃	22.5	2.25	0.90
MDC LiTaO ₃	5.8	0.58	0.23
100 cut 110 prop. GaAs	.2	X	X

Since values of F_Z range from -2 to +3.5 (see Table III) for different materials, impedance mismatch can be cancelled on at least some of the substrates. The "X's" in the table are values of h/λ where the thin electrode approximation is not valid.

The desired average value of \bar{F}_Z is obtained by choosing correct metal combinations (Eq. 11 and Table III). If the metal films have properties similar to bulk metals, the combinations shown in Table IX should produce a reflection-free single electrode structure. Electrode conductivity and fabrication considerations were not considered in the bimetal electrode design. Nevertheless, several practical combinations are projected and are boxed in Table IX. For example, a 1000 angstrom transducer made with 9% Cr, 92% Al on MDC LiTaO₃ at 845 MHz would, if all assumptions are reasonable, yield a zero impedance mismatch.

TABLE IX

Layer thickness percentages of
predicted reflection free bimetal single electrodes

	Total Electrode Thickness		
	$h/\lambda = .001$	$h/\lambda = .01$	$h/\lambda = .025$
ST Quartz	51%Cr 49%Au or 29%Cr 71%Ag	X	X
YZ LiNbO ₃	-	-	92%Cr 8%Al
37.95, X LiNbO ₃	-	73%Cr 27%Al or 60%Cr 40%Ti	7%Cr 93%Al
MDC LiTaO ₃	-	16%Cr 84%Au or 7%Cr 93%Ag	8%Cr 92%Al
100 cut 110 prop. GaAs	16%Cr 84%Au	X	X

X indicates that the thin electrode condition is not met

- indicates that no metals have been found to meet the conditions

C. Low Velocity Shift in Double Electrodes

The velocity shift produced by a bimetal double electrode is zero if

$$\bar{F}_V = -P_V \frac{k^2}{2} \frac{1}{h/\lambda} \quad (20a)$$

$$P_V = -1.71 \quad \text{at } \eta = .5 \quad (\text{Fig. 2b}) \quad (20b)$$

$$\bar{F}_V = \frac{.85 k^2}{h/\lambda} \quad (20c)$$

The \bar{F}_V required for nulling the velocity shift are tabulated for five substrates and three electrode thicknesses in Table X.

TABLE X
 \bar{F}_V required for zero DE velocity shift

	Electrode Thickness		
	$h/\lambda = .001$	$h/\lambda = .01$	$h/\lambda = .025$
ST Quartz	.47	X	X
YZ LiNbO ₃	39	3.9	1.56
37.95,X LiNbO ₃	51	5.1	2.0
MDC LiTaO ₃	6.5	.65	X
100 cut 110 prop.	.47	X	X
GaAs			

X indicates thin electrode condition is not met

Since the values of \bar{F}_V range from -6.64 to +1.74 for the metals considered, velocity shift of double electrodes on certain materials can be cancelled. The "X's" in the table are values of h/λ where the thin electrode

approximation is not valid.

The desired average value of \bar{W}_y is obtained by choosing different metal combinations (Eq. 11 and Table III). Assuming that the metal films have properties similar to bulk metals, the combinations shown in Table XI should produce a double electrode with zero velocity shift. Unfortunately, no obviously practical combinations were found. Bimetal electrodes with various combinations of Cr, Ag, Au, Ti, and Al were considered in the search for perturbation free electrodes. It may be possible that combinations of other metals may result in reduced perturbations. It is also possible that a metal used in conjunction with a dielectric may also reduce reflection and velocity shifts.

TABLE XI
Layer thickness percentages of
predicted zero velocity shift bimetal single electrodes

	Total Electrode Thickness		
	$h/\lambda = .001$	$h/\lambda = .01$	$h/\lambda = .025$
ST Quartz	89%Cr 11%Al	X	X
YZ LiNbO ₃	-	-	-
37.95,X LiNbO ₃	-	-	-
MDC LiTaO ₃	-	77%Cr 23%Al	X
100 cut 110 prop. GaAs	81%Cr 19%Au	X	X

X indicates that the thin electrode condition is not met

- indicates that no metals have been found to meet the conditions

Section V: Summary and Conclusions

This report provides a summary of the results of a theoretical analysis of the reflection and velocity shift of surface waves propagating in an array of electrodes. The results are given in terms of DELTERV and DELTERZ that can be used in the standard transmission line model used for transducer analysis. The impedance mismatch DELTERZ is described in terms of two constants P_Z and F_Z while the velocity shift DELTERV is given in terms of three constants P_Y , F_Y , S_Y . Analytical expressions are provided in this report for calculating P_Z , F_Z , P_Y and F_Y from material parameters. S_Y , describing energy storage effects, cannot be written in analytical form and is calculated from a numerical program.

The effect of neighboring environment on these constants has also been investigated. It is found that F_Y , F_Z are neighbor-independent and S_Y is only slightly neighbor-dependent. The correction factors for P_Z and P_Y in various neighbor configurations are provided.

The possibility of bimetal electrodes that minimize reflections or velocity shift has also been investigated and several practical combinations are provided.

REFERENCES

1. A. J. Slobodnik, Jr., K. R. Laker, T. L. Szabo, W. J. Kearns and G. A. Roberts, "Low sidelobe SAW filters using overlap and withdrawal weighted transducers," Proc. IEEE 1977 Ultrasonics Symposium, 77CH1264-1SU, pp. 757-762.
2. Supriyo Datta and Bill J. Hunsinger, "An analytical theory for the scattering of surface acoustic waves by a single electrode in a periodic array on a piezoelectric substrate," J. Appl. Phys. 51, 4817 (September 1980).
3. S. Datta and B. J. Hunsinger, "First order reflection coefficient of surface acoustic waves from thin strip overlays," J. Appl. Phys. 50, 5661 (August 1979).
4. S. Datta and B. J. Hunsinger, "Analysis of energy storage effects on SAW propagation in periodic arrays," IEEE Trans. on Sonics and Ultrasonics, to be published (November 1980, estimate).
5. S. Datta and B. J. Hunsinger, "A theoretical analysis of stored energy in surface wave gratings," Proc. IEEE 1979 Ultrasonics Symposium, 79CH1482-9, pp. 673-677.
6. S. Datta and B. J. Hunsinger, "A generalized model for periodic transducers with arbitrary voltages," Proc. IEEE 1978 Ultrasonics Symposium, 78CH1344-1SU, pp. 705-708.
7. S. Datta and B. J. Hunsinger, "Redefined element factor for simplified I.D.T. Design," Electronics Letters 14, 744 (November 1978).
8. A. L. Lentine, S. Datta, and B. J. Hunsinger, "Analysis of non-periodic transducers using a circuit model," IEEE Trans. on Sonics and Ultrasonics, to be published (November 1980, estimate).
9. A. L. Lentine, S. Datta, and B. J. Hunsinger, "Charge distribution for non-periodic transducers using a circuit model," Proc. IEEE 1979 Ultrasonics Symposium, 79CH1482-9, pp. 559-561.
10. Thomas L. Szabo, "Interdigital transducer models: design options," Proc. IEEE 1978 Ultrasonics Symposium, 78CH1344-1SU, pp. 701-704.
11. W. R. Smith and W. F. Pedler, "Fundamental- and harmonic-frequency circuit model analysis of interdigital transducers with arbitrary metallization ratios and polarity sequences," IEEE Trans. MTT 23, 953 (1975).
12. A. L. Lentine, "Analysis of non-periodic surface acoustic wave transducers and reflectors," M.S. Thesis in Electrical Engineering, University of Illinois, 1980. Also issued as CSL Report R-993.

13. B. J. Hunsinger and S. Datta, "Termination of surface acoustic wave velocity and impedance differences between metal strips and free surface regions of metallic gratings," Interim Report No. RADC-TR-81-4 to Rome Air Development Center, Air Force Systems Command, Griffiss Air Force Base, New York 13441, February 1981.
14. C. W. Chapman and T. W. Bristol, Acoustic Multistrip Device Techniques, Final Report ECOM-73-0276-F to U.S. Army Electronics Command, Fort Monmouth, New Jersey 07703.
15. Slobodnik, Conway and Delmonico, Microwave Acoustics Handbook, Volume 1A, Surface Wave Velocities, AD780172, National Technical Information Services, Springfield, Virginia 22151.
16. M. B. Schulz, B. J. Matsinger, and M. G. Holland, "Temperature Dependence of Surface Wave Velocity on α Quartz," J. of Appl. Phys. 41, 2755 (1970).
17. Kimio Shibayama, Kazuhiko Yamanouchi, Hiroaki Sato, and Toshiyasu Meguro, "Optimum Cut for Rotated Y-Cut LiNbO₃ Crystal Used as the Substrate of Acoustic-Surface-Wave Filters," Proc. of the IEEE 64, 595 (1976).
18. Andrew J. Slobodnik, Jr., José H. Silva, William J. Kearns, and Thomas L. Szabo, "Lithium Tantalate SAW Substrate Minimal Diffraction Cuts," IEEE Trans. on Sonics and Ultrasonics SU-25, 92 (1978).
19. R. H. Tancrell and F. Sandy, Analysis of Interdigital Transducers for Surface Acoustic Wave Devices, AD757485, National Technical Information Service, Springfield, VA 22151, March 1973.

APPENDIX: Finite Array Effects on Second Order Mechanical Scattering

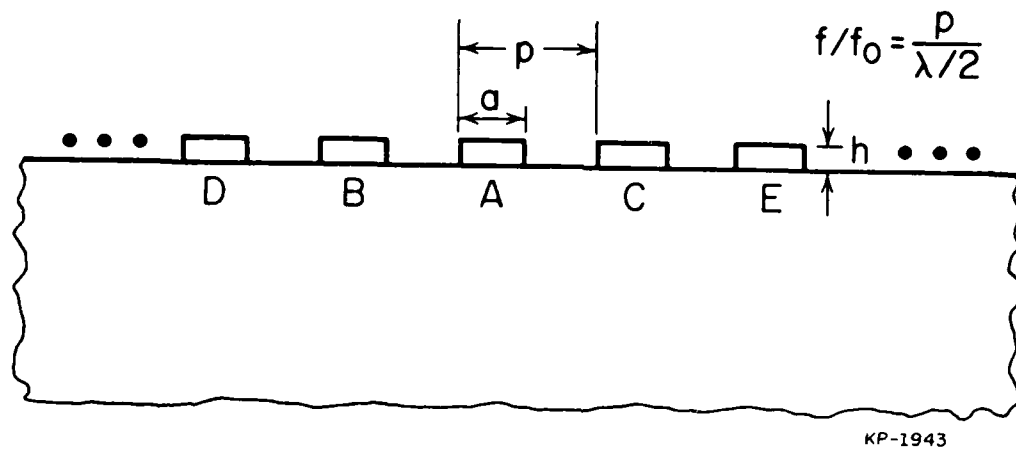


Fig. A1: An infinite array of electrodes

Consider first an infinite array. DV for electrode A is readily calculated from the infinite array analysis if four parameters are specified: a , p , h and f/f_0 ($= .5$ for double electrodes and 1 for single electrodes). To evaluate the effect of removing electrodes B and C on the DV for electrode A, we may use the infinite array analysis with the modification that p equals the spacing from A to E rather than the spacing from A to C. This means doubling p . Since the wavelength remains the same, we also need to double f/f_0 ; other parameters (a , h) remain the same.

Similarly, to evaluate the effect of removing electrodes D and E in addition to B and C, we treble p and f/f_0 keeping other parameters constant. In this way the effects of removing progressively distant neighbors is evaluated. The results are summarized in Table A1 for aluminum electrodes on ST-quartz.

Table A1

Effect of removing progressively distant neighbors on S_v
for aluminum electrodes on ST-quartz ($h/\lambda = .00125$)

Infinite Array	1.22
First N.N. removed	1.3
First and Second N.N. removed	1.28

It is seen that there is less than 10% change due to the removal of nearest neighbors. Since the accuracy of the program is estimated to be 10% this change may be neglected. Similar tests were run on several other substrate-electrode combinations with different h/λ , and the finite array effects were always found to be less than 12%, and usually between 4 and 8%.

MISSION
of
Rome Air Development Center

RADC plans and executes research, development, test and selected acquisition programs in support of Command, Control Communications and Intelligence (C³I) activities. Technical and engineering support within areas of technical competence is provided to ESD Program Offices (POs) and other ESD elements. The principal technical mission areas are communications, electromagnetic guidance and control, surveillance of ground and aerospace objects, intelligence data collection and handling, information system technology, ionospheric propagation, solid state sciences, microwave physics and electronic reliability, maintainability and compatibility.

N
DATE
ILME